

ENCLOSURE 4

TENNESSEE VALLEY AUTHORITY
SEQUOYAH NUCLEAR PLANT (SQN)
UNIT 2

Westinghouse Non-Proprietary Class 3
Application of W* to Sequoyah Unit 2 Steam Generator Tubes
February 2005

Application of W* Alternate Repair Criteria to Sequoyah Unit 2

February 2005

Westinghouse Electric Company LLC
P.O. Box 355
Pittsburgh, PA 15230-0355

© 2005 Westinghouse Electric Company LLC
All Rights Reserved

Application of W* Alternate Repair Criteria to Sequoyah Unit 2

See LTR-CDME-04-147 Revision 1 for the proprietary version

1.0 INTRODUCTION

TVA is proposing to modify the Sequoyah Unit 2 Technical Specifications 3/4.4.5, "Steam Generators," to change the scope of the steam generator (SG) tube sheet inspections required in the SG tubesheet region using the W* methodology. (W* is defined in WCAP-14797, Revision 2). Specifically, the proposed change will revise the Unit 2 Technical Specification definition for steam generator tube inspection included in Sequoyah Technical Specification (TS) Surveillance Requirement (SR) 4.4.5.4.a.8 to revise the definition to exclude the portion of the tube within the tubesheet below the W* distance. The proposed change will also revise SR 4.4.5.4.a.6 on steam generator tube repair criteria, add SR 4.4.5.2.e to require a 100 percent sample inspection of the hot leg tubesheet W* distance using an inspection probe qualified for detection of the expected degradation modes, add new W* terminology definitions in 4.4.5.4.a.11, and add new reporting criteria for W* inspection information in 4.4.5.5.d.1 and 4.4.5.5.e. The Sequoyah Unit 2 proposed change requires that any tube identified with service induced degradation in the W* distance or less than eight inches below the top-of-tube sheet (TTS), which ever is greater, must be repaired. Since Sequoyah proposes to repair any service induced degradation within the W* distance, this proposal is a conservative limited scope application of the complete W* methodology as described in WCAP-14797, Revision 2.

As a consequence of implementation, any degradation occurring below the W* distance may remain in service regardless of its axial or circumferential extent. The amendment will be based on portions of WCAP-14797-P, Rev. 2, entitled "Generic W* Tube Plugging Criteria for 51 Series Steam Generator Tubesheet Region WEXTEx Expansions," Reference 2.1, and the following information developed herein. The W* analysis accounts for the reinforcing effect that the tubesheet has on an external surface of the steam generator tubes within the tubesheet region.

This amendment is requested to address NRC GL 2004-01 with respect to defined tube inspection depth below the top of tubesheet using supplemental inspection techniques qualified for flaw detection in expanded tubesheet conditions, such as RPC or array probes.

2.0 W* BACKGROUND

Existing plant Technical Specification tube repair/plugging criteria apply throughout the tube length and do not take into account the reinforcing effect of the tubesheet on the external surface of an expanded tube. The presence of the tubesheet constrains the tube and complements tube integrity in that region by essentially precluding tube deformation beyond the expanded outside diameter. The resistance to both tube rupture and tube collapse is significantly enhanced by the tubesheet. In addition, the proximity of the tubesheet in the expanded region significantly reduces the leakage of throughwall tube cracks. Based on these considerations, the establishment of alternate repair criteria to the portion of tubing expanded by Westinghouse explosive tube expansion (WEXTEx) is supported by testing and analysis results included in Reference 2.1.

For Westinghouse Model 51 Series steam generators with WEXTEX expansions at Sequoyah Unit 2, the full depth tube-to-tubesheet expansion can be defined as follows. From the lower tube end and extending upward for a length of approximately 2.75 inches is a region expanded by a tube rolling expansion process. From the top of the rolled expansion region to the vicinity of the top of the tubesheet (TTS), the expansion joint was produced by the WEXTEX process. The resulting full depth tube-to-tubesheet expansion can be considered as four distinct areas. These are described in Reference 2.1 as:

1. The Roll Region – The region of tube which has been expanded by the tube rolling process. This region extends from the bottom of the tube to approximately 2.75 inches above the bottom of the tube.
2. The Roll Transition – The portion of the tube which extends from the roll expanded region of the tube to the initially unexpanded region, and which is subsequently expanded by the WEXTEX process.
3. The WEXTEX Region – The portion of the tube expanded by the explosive expansion process to be in contact with the tubesheet. This region starts at the roll transition and extends to the WEXTEX transition in the vicinity of the top of the tubesheet.
4. The WEXTEX Transition – The portion of the tube which acts as a juncture between the WEXTEX region and the unexpanded region of the tube. The region starts at the top of the explosively expanded region and extends for approximately 0.25 inches.

The alternate SG tube repair criteria referred to as W^* were developed by Westinghouse (and has been licensed to varying extents at another plants) to permit tubes with predominantly axially oriented primary water stress corrosion cracking in the WEXTEX and hardroll regions to remain in service. The W^* analysis determined the W^* length as measured from the bottom of the tube explosive expansion transition that would permit flaws below that length to remain in service and based on the assurance that adequate strength is available to resist the axial pullout loads experienced within the tubesheet during all plant conditions.

The following definitions apply with regard to describing the W^* criteria:

BWT – The bottom of the WEXTEX Transition as defined in WCAP-14797, Rev. 2, as approximately 0.25 inches from the top of the tubesheet.

W^* length – The maximum length of tubing below the bottom of the WEXTEX transition (BWT) which must be demonstrated to be non-degraded and is defined in WCAP-14797, Rev. 2, Section 4.0 as 7.0 inches below the bottom of the WEXTEX transition on the hot leg side.

W^* distance – The distance from the top of the tubesheet to the bottom of the W^* length including the distance from the top of the tubesheet to the BWT and measurement uncertainties.

The W^* analysis provides the basis for tubes with any form of degradation below the W^* length to remain in service. The presence of the surrounding tubesheet prevents tube rupture and

provides resistance against axial pullout loads during normal and accident conditions as discussed in Reference 2.1. In addition, any primary to secondary leakage from tube degradation below the W^* length is determined to be acceptably low as discussed in Section 4.0 of this report. Both steam generator tube structural and leakage integrity will be shown to meet the required performance criteria of Reference 2.2 and, thus, the necessary regulatory criteria as defined below.

General design criteria (GDC) 1, 2, 4, 14, 30, 31, and 32 of 10 CFR 50, Appendix A, define requirements for the reactor coolant pressure boundary (RCPB) with respect to structural and leakage integrity.

General design criterion (GDC) 19 of 10 CFR 50, Appendix A, defines requirements for the control room and for the radiation protection of the operators working within it. Accidents involving the leakage or burst of SG tubing comprise a challenge to the habitability of the control room.

10 CFR 50, Appendix B, establishes quality assurance requirements for the design, construction and operation of safety related components. The pertinent requirements of this appendix apply to all activities affecting the safety related functions of these components; these include, in part, inspecting, testing, operating and maintaining Criteria IX, XI and XVI of Appendix B as applied to the SG tube integrity program defined by NEI 97-06, Rev. 1 "Steam Generator Program Guidelines", Reference 2.2.

10 CFR 100, Reactor Site Criteria, established reactor-siting criteria, with respect to the risk of public exposure to the release of radioactive fission products. Accidents involving leakage or burst of SG tubing may compromise a challenge to containment and therefore involve an increased risk of radioactive release. Sequoyah Unit 2 is licensed for the use of an alternate source term in accordance with 10 CFR 50.67 for some design basis accidents.

Under 10 CFR 50.65, the Maintenance Rule, licensees classify steam generators as risk significant components because they are relied upon to remain functional during and after design basis events. SGs are to be monitored under 10 CFR 50.65 (a) (2) against industry established performance criteria. Meeting the performance criteria of NEI 97-06, Rev. 1, provides reasonable assurance that the SG tubing remains capable of fulfilling its specific safety function of maintaining the reactor coolant pressure boundary.

The SG performance criteria as defined in NEI 97-06, Rev. 1 (Reference 2.2) identify the standards against which performance is to be measured.

As discussed in more detail in Section 3.0 of this report, the generic W^* analysis contained in WCAP-14797, Rev. 2, is applicable to the Sequoyah Unit 2 SGs and defines the maximum hot leg W^* length for pullout resistance as 7.0 inches below the bottom of the WEXTEX transition. Seven (7.0 inches) is for Zone B. Note that although Zone A is 5.2 inches, 7.0 inches is applied throughout. The maximum NDE uncertainty on the W^* distance in Reference 2.1 is 0.12 inch. Therefore, the required Technical Specification inspection distance below the top of the tubesheet, or bottom of the WEXTEX transition, whichever is lower, is 7.12 inches

REFERENCES

- 2.1 WCAP-14797, Rev. 2, "Generic W* Tube Plugging Criteria for 51 Series Steam Generator Tubesheet Region WEXTEX Expansions," Westinghouse Electric Company, Madison, PA, March 2003 (Proprietary).
- 2.2 NEI 97-06, Rev. 1, "Steam Generator Program Guidelines," Nuclear Energy Institute, Washington, DC, January 2001.

3.0 APPLICABILITY OF WCAP-14797, REV. 2, TO SEQUOYAH UNIT 2

3.1 BACKGROUND INFORMATION

As noted above, the W^* length is the length of sound engagement of the tube within the tubesheet such that the force resisting expulsion from the tubesheet balances the force applied to the end of a presumed severed tube. The value of W^* is determined using applicable performance criteria relative to tube burst, expulsion from the tubesheet in this case, and relative to allowable leakage, relative to that established for alternate repair criteria (ARC). The structural performance criteria are that tube burst will not occur with a margin of 3 during normal operation and 1.4 during the most severe faulted event, a postulated steam line break (SLB) for Sequoyah Unit 2.

Applied Load

The applied force comes from the internal pressure in the tube. At the U-bend there is a component of the primary-to-secondary differential pressure acting in the axial direction. For the development of the criteria it is also assumed that the tube is severed in the tubesheet so that the differential pressure acts on the entire cross section area of the tube as calculated using the expanded outside diameter (OD) of the tube. The applied force, F_A , is determined from the applied pressure, ΔP , area, A , and the outside diameter, D_o , as

$$F_A = \Delta P A \text{ where, } A = \frac{\pi}{4} D_o^2 \quad (1)$$

Here, ΔP is the difference between the primary, P_P , and secondary pressure, P_S , at the top of the tubesheet, i.e., $P_P - P_S$.

Reaction Load

The reaction load in developing the W^* length arises from friction between the tube and the tubesheet within the tubesheet hole. The friction force is the product of the normal force between the tube and the tubesheet and coefficient of friction between the tube and the tubesheet. The normal force arises or is affected by four sources:

1. The residual preload from the expansion process,
2. Differential thermal expansion between the tube and the tubesheet,
3. Resultant pressure in the tube within the tubesheet, and
4. Dilation of the tubesheet holes from bowing of the tubesheet.

The first three items result in a compressive normal force between the OD of the tube and the ID of the tubesheet hole. The last item results in a reduction of the normal force near the top of the tubesheet and an increase in the normal force below the tubesheet neutral axis. It is noted that a lateral load applied to the center of the tube span above the TTS would tend to result in a slight lateral contraction in the axial direction. An analysis of the geometry of deflection shows that the

axial contraction is a small fraction of the lateral deflection and the bending load that would be developed at the top of the tubesheet would act to bind the tube tighter in the tubesheet hole. On this basis, the action of lateral flow loads can be neglected from further consideration.

*Determination of W**

The calculation performed is to find the length, W^* , that makes the following equality true between the resisting force on the left and the applied force on the right,

$$\mu (N_X + N_T + N_P + N_D) = \Delta P A \quad (2)$$

where

- N_X = The residual normal force from the expansion process,
- N_T = The normal force from the differential thermal expansion,
- N_P = The normal force due to the resultant pressure in the tube,
- N_D = The normal force resulting from dilation of the tubesheet hole,
- μ = The coefficient of friction between the tube and the tubesheet.

The resisting forces are due to the interface pressure between the tube and the tubesheet. The actual force is the product of the interface pressure times the effective area of contact, the circumference of the tube times the length of contact. Conservative uncertainty adjustments are then made to the length of contact to determine W^* . The diameter of the tube is constant, so an expression for the force per unit length is used and solved for the length, L . This means that each force term must be replaced by force per unit length term.

The solution for W^* is then,

$$W = \frac{\Delta P A}{\mu (F_X + F_T + F_P + F_D)} \quad (3)$$

where W stands for the W^* length and the letter F stands for the force per unit length of engagement. Each force per unit length term is then replaced by a corresponding pressure times circumference term, i.e.,

$$W = \frac{\Delta P A}{\mu (P_X + P_T + P_P + P_D) \pi D_o} \quad (4)$$

where D_o is the outside diameter of the expanded tube. Substituting for the cross section area yields,

$$W = \frac{\Delta P D_o}{4 \mu (P_X + P_T + P_P + P_D)} \quad (5)$$

for the determination of W , sans adjustments for uncertainties in measurement and end effects where the assumption of a severed tube has been made. The following points are to be noted:

1. The applied load term, the numerator is affected by changes in the operation of the plant. The value used for the generic document is the same as that for the plant specific application at Sequoyah Unit 2, hence the W^* length would be expected to be the same as that for the generic application.
2. The residual expansion pressure, P_X , is not affected by changes in the operation of the plant.
3. The thermal expansion term, P_T , is affected by changes in the hot leg temperature, T_{hot} . The hot leg temperature at Sequoyah Unit 2 is greater than the value used for the generic determination, hence the value of W^* for use at Sequoyah Unit 2 should be less than the generic value.
4. The differential pressure term, P_P , is affected by changes in the primary or secondary pressure. The differential pressure term used for the Sequoyah Unit 2 analysis is less than the generic analysis; therefore, the value of W^* for use at Sequoyah Unit 2 should be less than the generic value.
5. The dilation term, P_D , is also affected by changes in the primary or secondary pressure. The differential pressure acting across the tube sheet is the same as in the generic report. It is noted that different differential pressure conditions were used for the determination of the different contributing load terms for the analysis of the generic report. This is an acceptable approach since the structure remains elastic when the terms are superimposed and is discussed in the following section.

3.2 APPLICATION OF WCAP-14797-P, REV. 2, TO SEQUOYAH UNIT 2

The determination of the non-degraded tube length considers the residual preload capability of the tube expansion process, the thermal tightening effects due to thermal expansion coefficient differences between the tube and the tubesheet material, pressure tightening effects, and loss of preload due to tubesheet bow effects. The residual preload inherent in the expansion in the expansion process is independent of differences between analysis and plant conditions. The generic analysis uses a hot leg temperature of 590°F, whereas the limiting Sequoyah Unit 2 hot leg operating temperature is approximately 609.5°F (Reference 3.2). Therefore, the generic analysis includes less thermal tightening contribution than the actual condition within the steam generators. The generic analysis uses a secondary side steam pressure of 900 psia for evaluation of pressure tightening effects whereas the current secondary side steam pressure is 847.5 psig (1387 psi normal primary to secondary pressure differential). This steam pressure results in a smaller primary to secondary pressure differential for the generic analysis condition compared to the Sequoyah Unit 2 condition. Therefore, the generic analysis considers about 3.3% less pressure tightening contribution than the actual condition within the Sequoyah Unit 2 steam generators. The generic analyses also uses a steam pressure of 760 psia (1490 psi differential pressure across the tubesheet) for evaluation of tubesheet bow effects whereas the current Sequoyah Unit 2 differential pressure across the tubesheet is 1387 psi, thus the generic analysis is about 6.6% more conservative than the current Sequoyah Unit 2 conditions. Assumed normal

operating steam pressure also influences the analysis with regard to defining the applied end cap load that acts to push the postulated separated tube out of the tubesheet hole. The generic analysis uses a steam pressure of 760 psia for a differential pressure of 1490 psi which also is conservative compared to the current Sequoyah Unit 2 condition. Moreover, the internal steam pressure losses due to moisture separation will result in a slightly higher steam pressure within the steam generator. Therefore, the generic analysis includes greater end cap loading compared to the actual conditions within the Sequoyah Unit 2 steam generators. This end cap load must be reacted by the net residual contact load. As the end cap load is reduced, the non-degraded tube length is also reduced compared to the generic analysis.

Based on the above, it is expected that the Sequoyah Unit 2 specific W^* should be less than the generic value because of the net effect of the changes. The independent considerations lead to the results similar to those presented in the WCAP-14797, Rev. 2. Table 3.1 summarizes the comparison of Sequoyah Unit 2 operating parameters to those considered in the generic report.

3.3 SEQUOYAH UNIT 2 CONCLUSIONS

The Reference 3.1 determination of the W^* length of 5.2 inches Zone A and 7.0 inches for Zone B for the application to the Sequoyah Unit 2 SGs is considered to be valid. The differences in length required for the two zones are based on a variance in the tubesheet bow between peripheral and center regions of the tubesheet. The differences between the Sequoyah Unit 2 specific and the generic calculation values is the result of the conservative assumptions associated with performing a generic calculation, e.g., extremely low secondary side pressure (which increases the applied load and the dilation of the tubesheet holes), additional pressure considered in the crevice, and the use of a lower bound residual expansion pressure. Nevertheless, the application of W^* to the Sequoyah Unit 2 Nuclear plant (SQN2) SG tubes per the Reference 3.1 guidance is considered to be justified.

3.4 REFERENCES

- 3.1 WCAP-14797 (Proprietary) & WCAP-14798 (Non-Proprietary), Revision 2. *Generic W^* Tube Plugging Criteria for 51 Series Steam Generator Tubesheet Region WEXTX Expansions*. Westinghouse Electric Company, Madison, PA. February, 1997.
- 3.2 L29 041025 801, letter from M. H. Cothron (TVA) to W. K. Cullen (Westinghouse), 10/25/04.

Table 3.1 Comparison of W* for SQN2 SG Tubes Relative to Generic Information				
Item	Analysis Term & Description	Sequoyah Unit 2	Generic W*	Application of the Result
1	ΔP , Applied Pressure (End cap)	$P_s = 847.5$ psig (861.5 psia)	$P_G = 760$ psia	SQN2 W* < Generic W*
2	P_T , Thermal Tightening	$T_{hot} = 609.5^\circ\text{F}$	$T_{hot} = 590^\circ\text{F}$	SQN2 W* < Generic W*
3	P_P , Pressure Tightening	$P_s = 847.5$ psig (861.5 psia)	$P_G = 900$ psia	SQN2 W* < Generic W*
4	P_D , Dilation Loosening	?P = 1389 psi	?P = 1490 psi	SQN2 W* < Generic W*
5	F, Three times normal end cap load	$F_s = 2589$ lbf	$F_G = 2781$ lbf	SQN2 W* < Generic W*

4.0 STEAM LINE BREAK PRIMARY TO SECONDARY LEAKAGE DETERMINATION

This evaluation documents the primary water stress corrosion cracking (PWSCC) history of Sequoyah Unit 2 to establish that the most likely point of initiation is at the top of tubesheet, and that the PWSCC initiation potential below the top of tubesheet is significantly less than the top of tubesheet region. Evaluation of the SQN2 specific data indicates that the likelihood that a circumferentially separated tube exists below the current +Pt coil inspection distance of 8 inches below the top of tubesheet is exceptionally small.

This evaluation also establishes a conservative leakage allowance to be applied to the number of postulated circumferentially separated tubes in order to estimate steam line break condition leakage. The leakage allowance is established by evaluation of existing drilled hole leakage data of Reference 2.1 for varying crevice length conditions between the top of the sample (analogous to top of tubesheet) and hole locations, and then relating the contact pressure between the tube and stimulant collar to contact pressures within the actual SG tubes.

4.1 Estimate of the Number of Indications In Service Below the Current Tubesheet Region Inspection Distance of 8 Inches

PWSCC was first reported at Sequoyah Unit 2 at the EOC-4 (1990) inspection, four (4) axial PWSCC indications were reported. Circumferential PWSCC was first reported at the EOC-5 (1992) inspection in which two indications were reported along with 17 axial PWSCC indications at this outage. Circumferential PWSCC was not reported again until the EOC-8

(1997) inspection when 3 indications were reported. Axial PWSCC indications were reported at the EOC-6, EOC-7 and EOC-8 inspections. The 1996 inspection was the first application of +Pt inspection technology for the tubesheet region.

Through the EOC-10 (2000) outage the +Pt examination depth below the top of tubesheet (TTS) was 2 inches, i.e., the tube length between 2 and 8 inches below TTS was not previously inspected using a +Pt coil. Through the EOC-10 inspection with the inspection depth limited to 2 inches below the TTS, a total of 82 axial PWSCC indications (80 tubes) and 15 circumferential PWSCC indications (15 tubes) were reported. If the indication initiation distribution was uniform over the entire tube-in-tubesheet distance, then at least ninety-seven (97) indications would have been expected to be reported at the EOC-11 inspection in the distance between 2 and 5.5 inches below TTS since 97 indications were reported for all previous inspections. However, only 14 indications (9 axial, 5 circumferential) in 14 affected tubes were reported in this elevation range (2 to 5.5 inches below TTS) strongly implying that the distribution of indications is not uniform within the tubesheet and that the density of indications is skewed with the highest density near the top of tubesheet. Twelve (12) indications (11 axial, 1 circumferential) in nine (9) tubes were reported within 2 inches of TTS, for a total of 26 indications at the EOC-11 (2002) inspection. The remaining indications were between 2 and 7 inches below the TTS. These data strongly imply that the distribution of indications, and the potential for new indications, is not uniform within the tubesheet and is skewed with the highest number near the TTS.

For the EOC-12 inspection, 15 PWSCC indications were reported; 7 were reported in the previously inspected range from TTS to 5.5 inches below and 8 were reported at > 5.5 inches below TTS. These 8 indications located greater than 5.5 inches below TTS had never been previously inspected using a +Pt coil.

Figure 4.1 presents a cumulative distribution plot of elevations of all PWSCC indications reported at SQN2 and other plants with Series 51 SGs. Since elevation information is not available for the EOC-7 and earlier outages, the total number of indications reported from these outages were assigned to elevation bins based on the elevation distribution for the EOC-8 and later outages. This plot clearly shows that the PWSCC initiation potential is significantly greater for the top of tubesheet region than at deeper elevations. Recall that for the EOC-10 and all early outages, the +Pt inspection distance below TTS was 2 inches while for the EOC-11 and EOC-12 outages the +Pt inspection distances below TTS were 5.5 and 8 inches respectively. Figure 4.1 shows no increased initiation potential for indications at deeper elevations below TTS.

Figure 4.1 also presents cumulative distribution data of PWSCC as a function of elevation for the EOC-11 and EOC-12 outages only. For these outages, the inspection information for tube lengths never inspected can be used to formulate a judgment regarding indication potential at greater than 8 inches below TTS. At EOC-11, 26 total indications were reported with 14 located at greater than 2 inches below TTS, which was the bottom of the test extent for the EOC-10 outage. At EOC-12, 15 total indications were reported with 7 reported within 2 inches of TTS, zero reported between 2 and 5.5 inches below TTS (the bottom of test extent for the EOC-11 outage), and 8 reported at greater than 5.5 inches below TTS. The lack of new initiates in the 2 to 5.5 inch below TTS range for the EOC-12 outage suggests a limited initiation potential for

indications below the expansion transition. For both of these inspections, the inspection transient effect, which applies to the indication totals for areas never before inspected, shows that the total number of indications is approximately split between new initiates and indications never before inspected. Therefore, the historical indication counts can be used to estimate the number of indications below the EOC-13 inspection distance.

The elevation distributions for all data and the EOC-11/EOC-12 data are quite similar, further supporting the argument that PWSCC initiation potential below the transition region is far less than for the transition region. Note that for these plots, indication elevations between 0.00 and 0.99 inch below the top of tubesheet are found in the 0 inch bin. The SQN2 cumulative elevation distribution was compared against that of other plants with Model 51 SGs. The distributions for all plants are quite similar. Figure 4.1 also includes the Diablo Canyon Power Plant and Beaver Valley Power Station distributions which are similar to SQN2.

For the EOC-11 and EOC-12 outages with a +Pt inspection distance of 5.5 and 8 inches below TTS respectively, 41 PWSCC indications were reported; 19 were reported within a previously inspected distance. For the EOC-4 through EOC-12 outages, 138 indications were reported with 124, or 90%, within 4 inches of the top of tubesheet and 10% reported greater than 4 inches below TTS. Thus, the number of indications between 8 and 12 inches below TTS would not be expected to be greater than the number reported between 4 and 8 inches below TTS. For conservatism in assessing the potential for leakage from indications below the inspection distance, 25% of the total historical plus EOC-13 projected indication count will be assumed to reside between 8 and 12 inches below TTS while only 10% of the historical total reside within a 4 inch length from 4 to 8 inches below TTS.

To date, 138 total indications have been reported, only 25, or 18%, of which were circumferentially oriented. Figure 4.2 illustrates the individual indication totals by outage. A regression analysis using all of the data suggests that approximately 23 indications are expected for the EOC-13 outage. Using only data from the last four outages, 25 indications are anticipated. Therefore, the cumulative SQN2 total number of indications including the EOC-13 projection is a maximum of 163 (138 plus 25). Figure 4.3 plots cumulative PWSCC totals for SQN2 by outage. This data shows the cumulative PWSCC trending to be linear. Based on the cumulative data, only 12 indications would be expected at EOC13. Therefore, use of the mean fit to the most recent outage data (Figure 4.2) represents a conservative estimate of EOC13 indications. An additional 41 indications (25% of combined historical indications plus EOC-13 new indications) might be observed if the inspection distance were increased from 8 to 12 inches below TTS. A very small number of these 41 postulated indications between 8 and 12 inches below TTS would be expected to have all of the following characteristics;

1. be circumferentially oriented
2. represent a 100% throughwall (TW) condition, and
3. extend for 360° (circumferential cracks).

At the EOC-12 inspection in 2003, which was the first inspection to 8 inches below TTS, four circumferential indications were reported; three were located at the WEXTEx expansion transition and one was located at 9.8 inches below TTS. As the length of tubing from 5.5 to 8

inches below TTS had never been inspected using a +Pt coil, it would be expected that a modest number of large voltage indications would be observed in this range. None of these four were representative of a 100% TW condition based on the +Pt amplitude and the longest circumferential flaw arc length, i.e., 46°. Eleven axial PWSCC indications were reported, of which seven were located at > 5.5 inches below TTS and were not previously inspected. Only one of the EOC-12 axial indications represented a 100% TW degradation potential based on flaw amplitude. Therefore, for the 41 postulated indications between 8 and 12 inches below TTS, seven (18% of 41) would be expected to be circumferentially oriented, and the number of indications with 100%TW penetration over 360° is zero. The 25 circumferential indications reported to date were located between the expansion transition and 9.8 inches below TTS; only two were located at > 4 inches below TTS. The longest circumferential PWSCC arc length reported for all outages was 97° at the EOC-11 outage.

Figure 4.4 presents a tubesheet map plot of all Unit 2 PWSCC indications reported at EOC-8 and later. A total of 22 of the 82 indications in this population are reported to be in the outboard region, defined as Zone A, which is the zone with the lesser amount of tubesheet deflection during operating or faulted conditions.

The above data were developed using the nominal inspection distance below TTS of 2, 5.5, or 8 inches, based on the outage chronology. In actuality, the inspection distance applied to each tube exceeds the specified value. This is purposely done during the data collection process to ensure that the appropriate distance is examined. This is shown by the deepest reported indications which reside at about 9.5 inches below TTS. Figure 4.5 presents a plot of the binned PWSCC elevation data for all historical indications with and without the expansion transition indications. Excluding the expansion transition indications would be expected to provide the best dataset for estimating indications at deeper depths. A best fit regression of the data with the expansion transition excluded is included in this plot. This plot shows that the predicted number of indications in each bin is only 1 for 1 inch increment bins greater than 11 inches below TTS.

Figure 4-5 also includes an upper 90% probability prediction bound for this data. The 95% prediction suggests approximately 27 indications would be expected at > 8 but < 12 inches below the TTS. For conservatism, the previously established value of 41 will be applied. The binned indication count data for the EOC-11 and EOC-12 outages shows the largest number of indications in any 1 inch bin below the expansion transition was only 4. Therefore, there is no basis to assume that large numbers of indications are present below the inspection depth.

Note that this analysis is provided to estimate the number of indications between 8 and 12 inches below TTS using existing data. The EOC-13 outage inspection data will be evaluated in the same manner to more accurately assess the postulated number of indications between 8 and 12 inches below TTS.

Previous evaluation of the residual stress distribution in hydraulically expanded tube-in-tubesheet joints indicates that the residual stresses below the expansion transition are likely compressive in nature. Therefore, PWSCC initiation is likely associated with a localized geometry discontinuity resultant from the tube drilling process. As all tubesheet holes were drilled from the primary face, the frequency of tube hole abnormalities would be expected to be increased as the

secondary side face of the tubesheet is approached. The data of Figure 4.1 supports this argument. Furthermore the circumferential extent of these abnormalities would be expected to be limited. The inspection data that shows the largest circumferential arc extent is 38° for indications below TTS also supports this assumption.

4.2 Leakage Potential Evaluation of Postulated Circumferential Degradation Below W*

The NRC Staff has recently questioned the validity of the original assumption presented by WCAP-14797, Rev. 2, that postulated circumferential degradation below W* would not produce leakage at SLB conditions. This section establishes a basis supporting the argument that meaningful leakage would not result from degradation below the W* elevation. The accuracy of this statement can also be qualitatively verified by examining operating plant history. SG leakage events have been attributed to ODS/CC in the freespan and at TSP intersections, PW/SCC at U-bends, at tack roll transitions of non-expanded tubes, and due to loose parts/foreign objects. Therefore, as no operating experience has been associated with postulated circumferential degradation below W*, it is reasonable to assume that the potential for such indications is unlikely, or that the inherent leakage resistance of at least 7 inches of sound WEXT/EX expansion (based on a nominal 8 inch below TTS inspection distance when the expansion transition distance is ignored) at TTS is sufficient to preclude reportable leakage (i.e., < 2 gpd or < 1.4·10⁻⁴ gpm).

Two sets of leakage data support the W* criteria. The first set of data was prepared by tack rolling a 7/8 inches OD by 0.050 inch wall thickness Alloy 600 tube into a carbon steel collar. The tube was then seal welded to the collar and then WEXT/EX expanded. Ten (10) 0.125 inch diameter holes were drilled through the collar and tube at elevations referenced from the top of the test collar. The second set of leakage data examined the impact of contact pressure upon crack opening potential for axial flaws. This data may not be directly applicable to postulated circumferential degradation but it does show that at about 2500 psi contact pressure that leak rates are essentially zero, i.e., < 1.33·10⁻⁵ gpm. These tests located the upper crack tip immediately below a channel machined in the tubesheet collar to eliminate any potential for flow restriction. The prevention of leakage at this contact pressure is expected to be independent of flaw orientation as contact pressure exceeds the primary to secondary pressure differential.

For the first set of leakage data, if it is assumed that the entire circumference of the drilled holes contributes to the leakage flow, the effective leakage flow length was 3.93 inches which is greater than the leakage flow length of a postulated circumferentially separated tube of 2.79 inches based on a tubesheet hole ID of 0.890 inch. The first set of holes was located at 3 inches from the top of the test collar thus resulting in a tube to collar contact length of < 3 inch due to the transition geometry. The through holes in the carbon steel collar were drilled to a diameter slightly larger than 0.125 inch to permit staking of the tube holes. This staking operation inwardly deformed the tube at the tube/collar interface, in effect pulling the tube from the collar at the hole to ensure that the drilling operation did not affect the leak path. For this set of tests, the leak rate at 600°F was essentially 0 at SLB pressure differential. For these samples tested at 600°F and a pressure differential of 1620 psi, leak rates were essentially identical to the 2650 SLB tests suggesting that the increased driving pressure was balanced by the increased contact pressure due to pressure expansion. The observation of leakage at normal operating conditions

in the leakage samples is not consistent with operating plant experience, either the samples yield conservative leakage estimates or such degradation is not present in operating units. A choked flow condition may have also been present which implies that increased expansion distance between the indications and top of tubesheet would further reduce leak rate by adding additional resistance to flow. After completion of the 3 inch tests, a new set of holes was drilled at 2 inches from the top of the test collar. Leak rates were elevated above the 3 inch test levels. This process was repeated again locating the holes at 1.25 inches below the top of the collar and leak rates were again elevated above the previous test levels. The tube holes were not plugged after completion of testing at the 3 inches and 2 inches nominal crevice tests. Thus, the 1.25 inches and 2 inches nominal tests included leakage effects of the holes below these elevations.¹ In effect, the 1.25, 2, and 3 inches nominal crevice tests simulated tubes with circumferential separations at 7.7, 9.5, and 10.3 inches below TTS respectively when based on the contact pressures presented in Figure 4.8, which were conservatively taken from the values developed for pullout load analyses as listed in Table 4.3-9 of WCAP-14797, Rev 2. The use of the contact pressures developed for leak rate analysis and presented in Table 4.3-11 of WCAP-14797 would yield equivalent depth of about 1 inch less than those listed above. Using the above values result in an increase in the margin relative to contact pressure of about 500 psi. All of these tests were conducted at a temperature of 600°F. The inherent WEXTEx expansion contact pressure is not included in the values of Figure 4.8.

Prior to elevated temperature testing, room temperature testing was conducted at 1620 psid for each of the crevice depth conditions. For the room temperature, 3 inch tests at 1620 psid, the average leak rate was ~100 times the 600°F average leak rate. Figure 4.6 presents the 600°F drilled hole leak rate test data as a function of crevice depth for 2650 psid. Figure 4.7 presents the 600°F drilled hole leak rate test data as a function of crevice depth for the 2650 psid and 1620 psid test conditions. For the 3 inch nominal crevice tests at 2650 psid, the actual crevice depths were 2.37 inches, 2.29 inches, 2.37 inches, and 2.1 inches, for an average crevice depth of 2.28 inches. For the 2 inch nominal crevice tests, the average crevice length was 1.28 inches, and for the 1.25 inches nominal crevice tests, the average crevice length was 0.61 inches.

For the 3 inch tests at 600°F, 2 of the 4 samples had no leakage at 1620 or 2650 psid. The leak rates of the other two 2650 psid samples were $1.33 \cdot 10^{-6}$ gpm and $1.33 \cdot 10^{-5}$ gpm. For these tests, radial contact pressure due to thermal expansion, pressure expansion, and WEXTEx expansion are inherent. There was no allowance for tubesheet hole dilation. Thus, these tests can be seen as a representation of the point where tubesheet hole dilation effects are neutral, i.e., at the neutral axis, or between 11 and 12 inches below the TTS.

The above developed upper 90% prediction leak rates of $4.5 \cdot 10^{-3}$ gpm per tube for indications between 8 and 12 inches below TTS and $8.7 \cdot 10^{-5}$ gpm per tube for indications >12 inches below TTS are developed using data for those specimens that leaked. Note that 2 specimens with 3 inch nominal crevice lengths did not leak. If a leak rate of $7 \cdot 10^{-6}$ gpm, which is the average leak rate of the 3 inch nominal specimens that leaked is applied to the zero leakage specimens the upper 90% prediction is reduced by a factor of 1.3 (see Figure 4.6). If a leak rate of $1.33 \cdot 10^{-6}$ gpm, which is the lowest leak rate of the 3 inch nominal crevice specimens is applied to the zero

¹ This would be expected to be small because of the lack of a pressure drop between the holes.

leakage specimens the upper 90% prediction is reduced by a factor of 2.7 (see Figure 4.6). Figure 4.6 also shows the dependence of the leak rate on crevice depth, e.g., any postulated leakage from a separated tube at 18 inches below TTS (which would include increasingly greater contact pressure with increasing depth below TTS) would be much lower than the applied value which is based on a depth of 12 inches below TTS.

Figure 4.8 presents a plot of contact pressure as a function of distance below TTS for 4200 seconds into the SLB event. At this point the primary and secondary side temperatures are assumed to be constant, and tubesheet bow effects are maximized. The contact pressures in the drilled hole specimens are similar to the predicted contact pressures in the tube for depths of about 7.7 to 10.3 inches below TTS. WEXTEx expansion contact pressures for the tube and leakage specimens are not included in this plot. Calculation of tube contact pressures assumes a crevice pressure of 800 psi, which reduces the contact pressure due to pressurization. Contact pressure calculation for the leakage specimens assumes no pressure within the crevice, which conservatively estimates contact pressure for the leakage specimens. With assumed secondary side pressures within the crevice the contact pressures for the 3 inch nominal specimens could be as low as 1514 psi.

WCAP-14797, Rev. 2, calculates the total positive radial contact pressure as a function of depth below top of tubesheet due to thermal expansion, pressure expansion, and WEXTEx expansion. The reduction in contact pressure due to tubesheet bow is included to develop resultant radial contact pressure as a function of depth below the top of tubesheet. Figure 4.8 presents a plot of resultant radial contact pressure as a function of depth below top of tubesheet for the Zone A and B regions, excluding WEXTEx residual contact pressure of 693 psi, at 4200 seconds into the SLB event. If the Zone B data is conservatively applied to the entire tubesheet, at approximately 10.8 inches below TTS, the resultant radial contact pressure is 2500 psi.

Figure 4.8 shows that the drilled hole test contact pressures are higher for the actual crevice lengths tested compared to the resultant plot of contact pressure for a tube at the same crevice depth condition. The 1.25 inches nominal crevice tests involve a contact pressure consistent with the Zone B tube at approximately 7.7 inches below TTS and the 3 inch nominal crevice tests involve a contact pressure consistent with the Zone B tube at approximately 10.3 inches below TTS. The rate of change of contact pressure as function of distance below TTS is more rapid for the drilled hole specimens than for the actual tube. For the 1.25 inch nominal crevice test case, an actual crevice length of ~0.6 inch with positive contact pressure was provided. The corresponding tube would have a crevice of ~4 inches with positive resultant contact pressure for ~3.5 inches above a postulated separation. Thus, it could be argued that the drilled hole specimen data is conservative compared to the actual tube in the range of 7.7 to 10.3 inches below TTS due to the more rapid change in contact pressures as a function of distance below TTS and shorter crevice length with positive contact pressure. However, since the contact pressure reduction due to hole dilation was not included, a conservative estimate of potential leak rate for a postulated circumferentially separated tube below the W^* inspection distance of 8 inches below TTS would be to use the predicted leak rates. At this crevice depth (equivalent to leakage specimens with actual crevice depth of 0.61 inch), the predicted leak rate is $1.9 \cdot 10^{-3}$ gpm using the mean (arithmetic average) regression of the leak rate as a function of actual crevice depth and $4.5 \cdot 10^{-3}$ gpm at the upper 90% prediction bound, see Figure 4.6. Thus, the SLB

condition conservative leak rate applied to a circumferentially separated tube between 8.0 and 12 inches below TTS is $4.5 \cdot 10^{-3}$ gpm. For a postulated circumferentially separated tube at > 12 inches below TTS, substantial contact pressure and crevice lengths would exist above this location, resulting in a no leakage condition. However, a conservative leakage allowance will be included.

It is noted that the leak rate data are independent of the test pressure for the lengths tested since fitting separate regression lines yields similar slopes and intercepts. Statistical comparisons were made of the results of such analyses and it was found that there were no statistically meaningful differences. Thus, the attendant increase in contact pressure compensated for the increase in pressure difference by reducing the area available for the leakage flow, or the flow in the test specimen crevices was at choke conditions. Regardless, the conclusion is that all of the leak rate data, i.e., those for 1620, 2000 and 2650 psid, could have been included on the same plot. Performance of this analysis results in a similar regression line that predicts slightly lower median flow rates. The other consequence of including all of the data is a reduction in the standard error of the regression and a reduction in the 90th percentile prediction bound, about a factor of two or slightly greater over the range of interest. Thus, the above calculation is based on a conservative segregation of the data. In addition, finally, additional calculations were performed to obtain linear regression coefficients for the logarithm of the leak rate as a function of the crevice length and the calculated contact pressure. The regression results were then used to estimate the 90th percentile prediction bound relative to the predictions based on the regression on crevice length alone. The results indicated that neglecting the contact pressure leads to over predictions on the order of 4 to 20 relative to that from using the combined data set. In conclusion, the bounding calculation results reported could be about an order of magnitude greater than would be obtained from a refinement of the analysis.

As no 100% TW, 360° circumferentially separated tubes are anticipated to be present between 8 and 12 inches below TTS, application of the W* alternate repair criteria could be such as to not involve leakage from postulated indications below W*. No leakage would be expected due to the substantial contact pressure at greater than 12 inches below the top of tubesheet. However, for practical purposes an estimate can be made and is discussed in developing a conservative estimate of the potential leakage as follows:

- 1) If it is assumed that all 41 postulated indications between 8 and 12 inches below the TTS are circumferentially oriented and the tubes are severed, the leakage associated with these indications is 0.18 gpm using the 90th percentile leak rate corresponding to a test specimen crevice length of 0.61 inch which has a contact pressure similar to that in the SG at a depth of ~8 inches, and would be dispersed over 4 SGs.
- 2) A conservative estimate of leakage for indications at greater than 12 inches below TTS can be accomplished by applying the upper 90th percentile prediction leak rate at 2650 psid for the 3 inch nominal crevice data of $8.7 \cdot 10^{-5}$ gpm. The contact pressure for the 3 inch nominal crevice samples is approximately equal to a Zone B at 10 inches below the TTS. At 12 inches below the top of tubesheet, the expected Zone B contact pressure at 4200 seconds into the SLB event is approximately 2900 psi, about

600 psi greater than for the average of 2273 psi for the 3 inch nominal crevice length leakage specimens.

If all remaining active tubes in the least plugged SG are assumed to contain a circumferential separation at 12 inches below TTS, the SLB leakage contribution would be approximately 0.26 gpm (3000 tubes times $8.7 \cdot 10^{-5}$ gpm per tube). Note that 2 of the 4 samples had no leakage at 2650 psid and the constrained crack leak test data suggest that no leakage could be expected, regardless of the indication orientation at a contact pressure of greater than 2500 psi.

Zone A contact pressures as a function of depth below the top of the tubesheet are higher than for Zone B to a depth of about 11 inches. The increase in contact pressure above that depth can have a significant effect on the leak rate, however, this has been conservatively neglected in the leak rate analysis. Zone A tubes retain positive resultant contact pressure for almost the entire crevice length. The added length with positive contact pressure is expected to provide a substantially increased resistance to leakage during a postulated event. It should also be noted that the assumption that all tubes contain a circumferential separation at > 12 inches below TTS is an extreme conservatism.

Combining the upper 90% prediction leak rate with the assumption that all tubes are separated is even more conservative, and may be so conservative that the predicted value is unrealistic. For a large number of samples, i.e., assuming all tubes are separated, any postulated SLB condition leakage would be expected to migrate to the mean leak rate. The mean, i.e., arithmetic average, leak rate regression for the 3 inch nominal crevice length specimens is on the order of $1.6 \cdot 10^{-5}$ gpm per tube, and for the conservative assumption of all tubes separated, the expected leak rate would then be about 20% of the value of 0.26 gpm calculated above.

Summarizing, for an EOC-13 nominal inspection distance of 8 inches below TTS, total SLB leakage from indications below the inspection distance could be 0.44 gpm, with 0.18 gpm attributed to indications between 8 and 12 inches below TTS and 0.26 gpm attributed to indications at greater than 12 inches below TTS.

Predicted leak rate as a function of contact pressure was also considered, however it was determined that the leak rate prediction is best accomplished using the specimen crevice depth. This determination was based on a comparison of the statistical goodness-of-fit between the two sets of data. At equal probability levels, the estimation of leakage using crevice depth provides for a conservative total leakage prediction compared to estimation of leakage using contact pressure.

Additional conservatism is present in the above described leakage prediction since all indications below the EOC-13 planned inspection depth of 8 inches below TTS are assumed to be circumferentially separated. As stated above, only 10% of the total historical indication count are circumferentially oriented. Leakage estimation from axial PWSCC is substantially less than the model used for circumferentially oriented PWSCC.

4.3 Confirmatory Leak Rate Evaluation

In order to partially quantify the conservatism associated with the first order linear regression analysis approach involving only the crevice length, a subsequent analysis was performed which included the contact pressure as a second variable. The analysis also considered all of the data in establishing the regression line. The results of the analysis are presented on Figure 4.9. The 90th percentile leak rate for a crevice depth of 0.61 inch is $5.24 \cdot 10^{-4}$, corresponding to the value of $4.4 \cdot 10^{-3}$ from the single variable analysis, a difference of a factor of 8. Likewise, the bounding leak rate for a crevice length of 2.28 inches was calculated to be $1.33 \cdot 10^{-5}$, a factor of 6.5 less than the corresponding value from the single variable analysis.

Application of these results to the previous analyses leads to the expectation that the 0.18 gpm total leak rate from indications in the range of 8 to 12 inches below the TTS would be reduced to 0.015 gpm by increasing the complexity of the analysis. Similarly, the 0.26 gpm leak rate for 3,000 postulated separated tubes at a depth of 12 inches would be reduced to 0.04 gpm, with the total expected leak rate being about 0.055 gpm instead of the considered 0.44 gpm. The calculated median leak rate per tube used with the assumption that all of the tubes in the SG are severed is reduced from $4 \cdot 10^{-6}$ to $4.3 \cdot 10^{-7}$ gpm per tube.

4.4 Conclusions Regarding Leakage Testing

The WEXTEx drilled hole leakage testing indicates the following characteristics for a WEXTEx expanded tube with a postulated circumferential separation below the W* inspection distance.

1. Comparison of the room temperature and elevated temperature tests indicates that elevated temperature leak rates were approximately 100 times less than room temperature leak rates.
2. Comparison of the elevated temperature test data for 1620 and 2650 psi pressure differential shows the leak rates are essential constant for both pressure differential conditions suggesting that pressure expansion has a limited effect on leak rates.
3. Based on the observations of items 1 and 2, contact pressure is seen as the most significant factor for restricting leak rate.
4. For the 1.25" nominal crevice test case, the contact pressure is approximately equal to the contact pressure of an expanded tube at 7.7" below TTS while for the 3" nominal crevice test case, the contact pressure is approximately equal to the contact pressure of an expanded tubes at 10.3 inches below TTS. The contact pressure reduction in the test samples was more rapid (per unit length) than in the actual tube. Contact pressures in the leakage specimens did not account for pressure within the tube to tubesheet crevice, and results in a conservative estimate of contact pressure. Contact pressures for the SG tube (Figure 4.8) includes a crevice pressure of 800 psi for a leakage condition.
5. The accumulation of the leakage effects of the holes at 2 and 3 inch below TTS can be seen as a representation of the postulated case where the tube is separated at 7.7, 9.5, and 10.3 inch below TTS. The leak rate determined for the 1.25 inches nominal crevice tests is a conservative estimate of leakage for a tube with a postulated circumferential separation below the W* inspection distance.

6. Evaluation of the reported flaw elevations for SQN2 shows that indications were reported as deep as 9.8 inches below TTS. Therefore, a number of tubes were inspected to depths exceeding the nominal inspection depth for EOC-12 of 8 inches below TTS. Therefore, the likelihood of any postulated circumferentially separated tube at or below 8 inches below TTS is exceptionally small.
7. Zone B tubes were used for estimation of SLB condition leak rates. The Zone A tubes retain positive resultant contact pressure over the entire crevice length, and this increased length is expected to represent a significant decrease in SLB condition leak rates compared to Zone B.

Figure 4.1

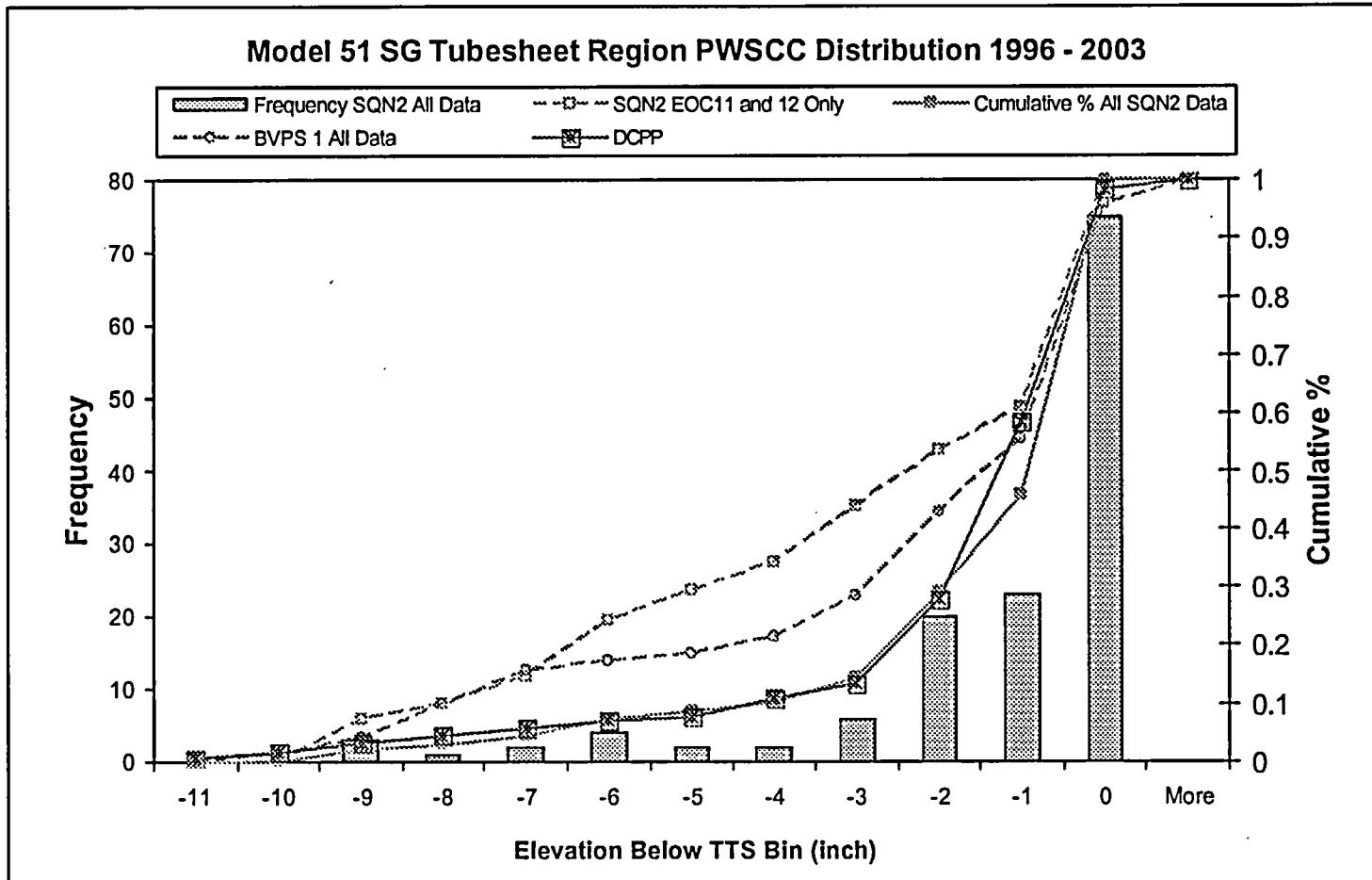


Figure 4.2

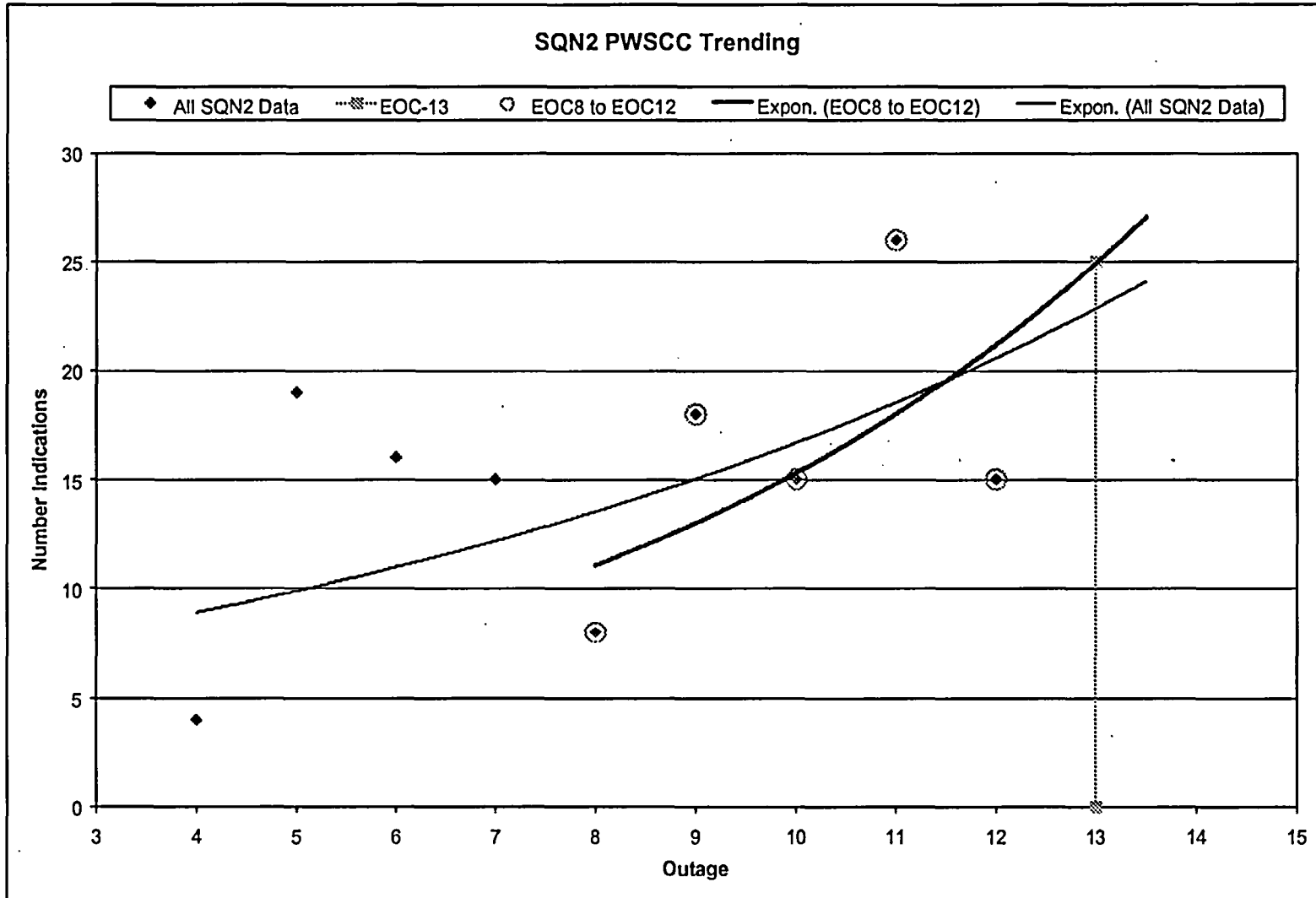


Figure 4.3

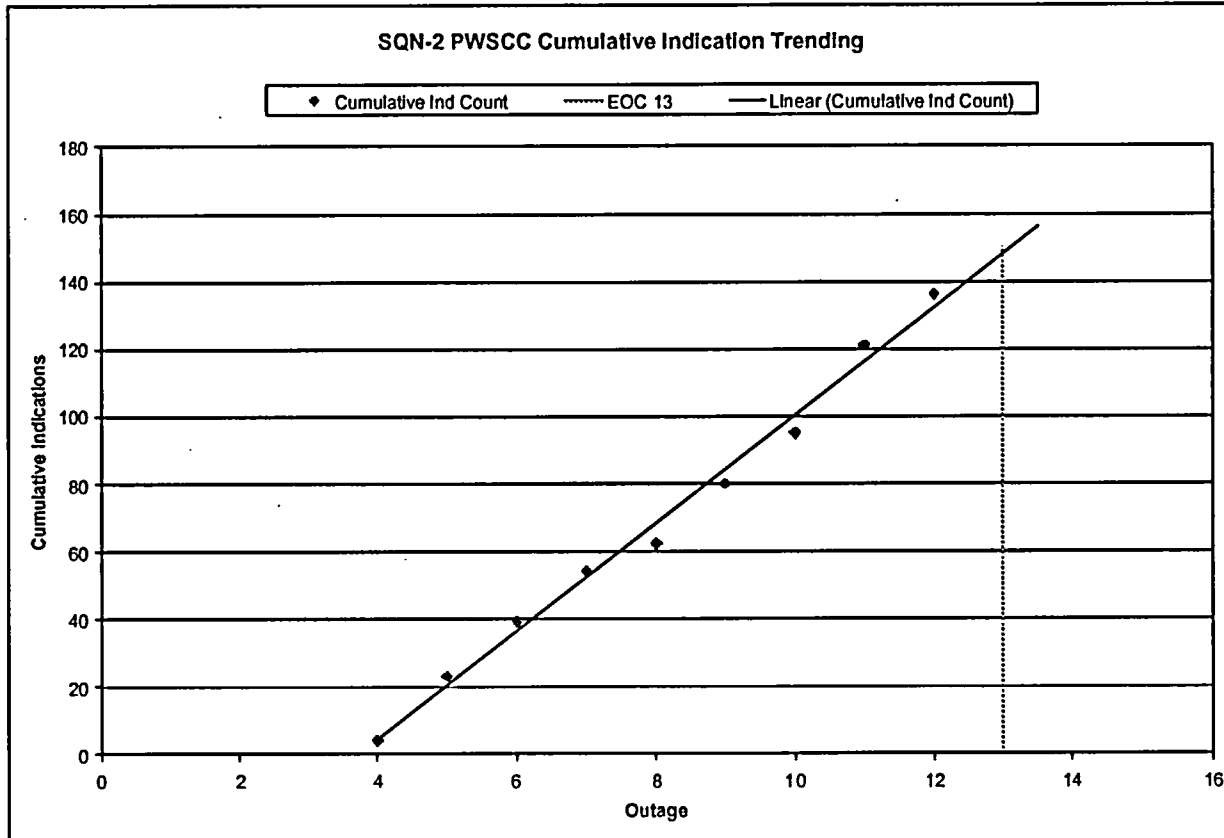


Figure 4.4

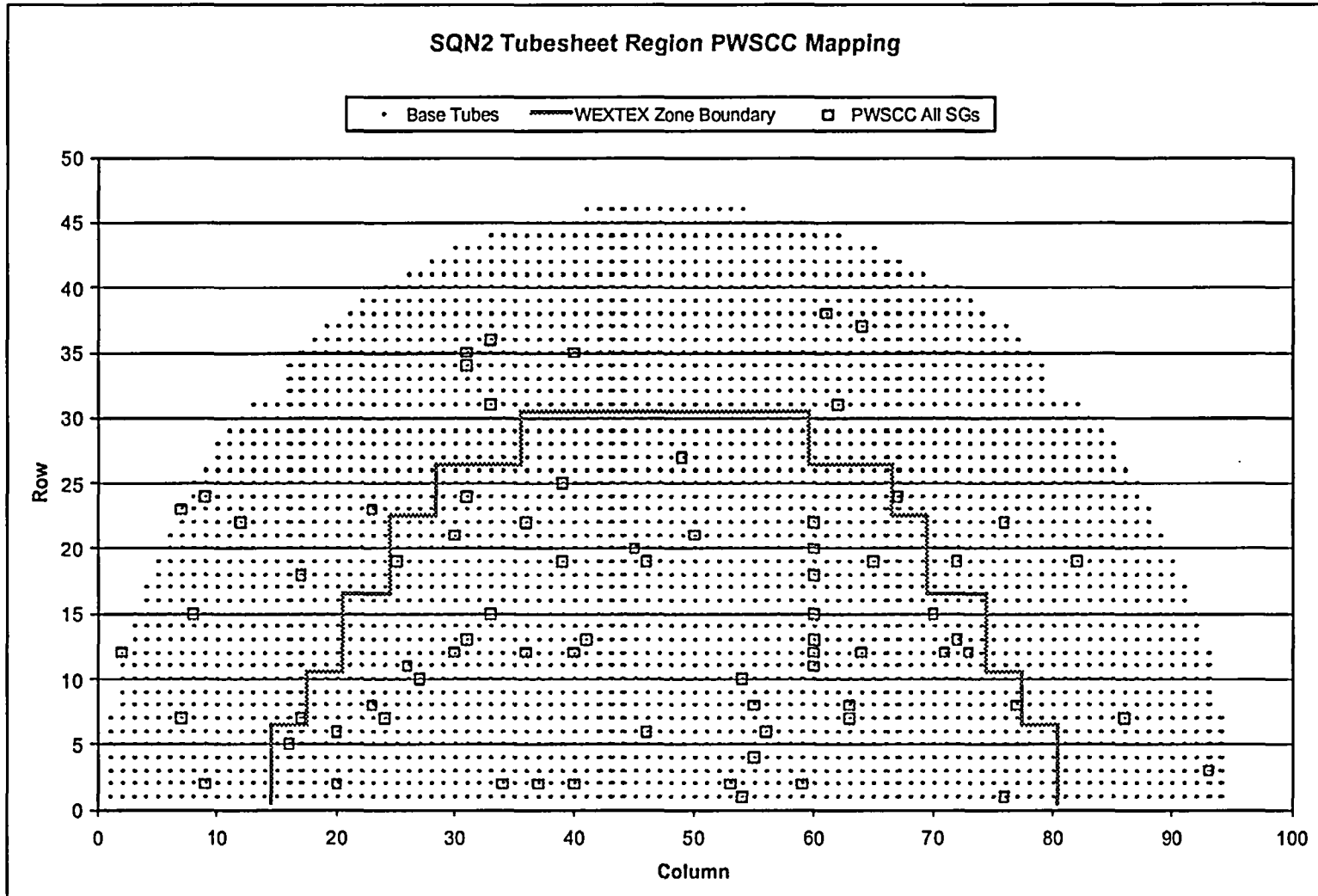


Figure 4.5

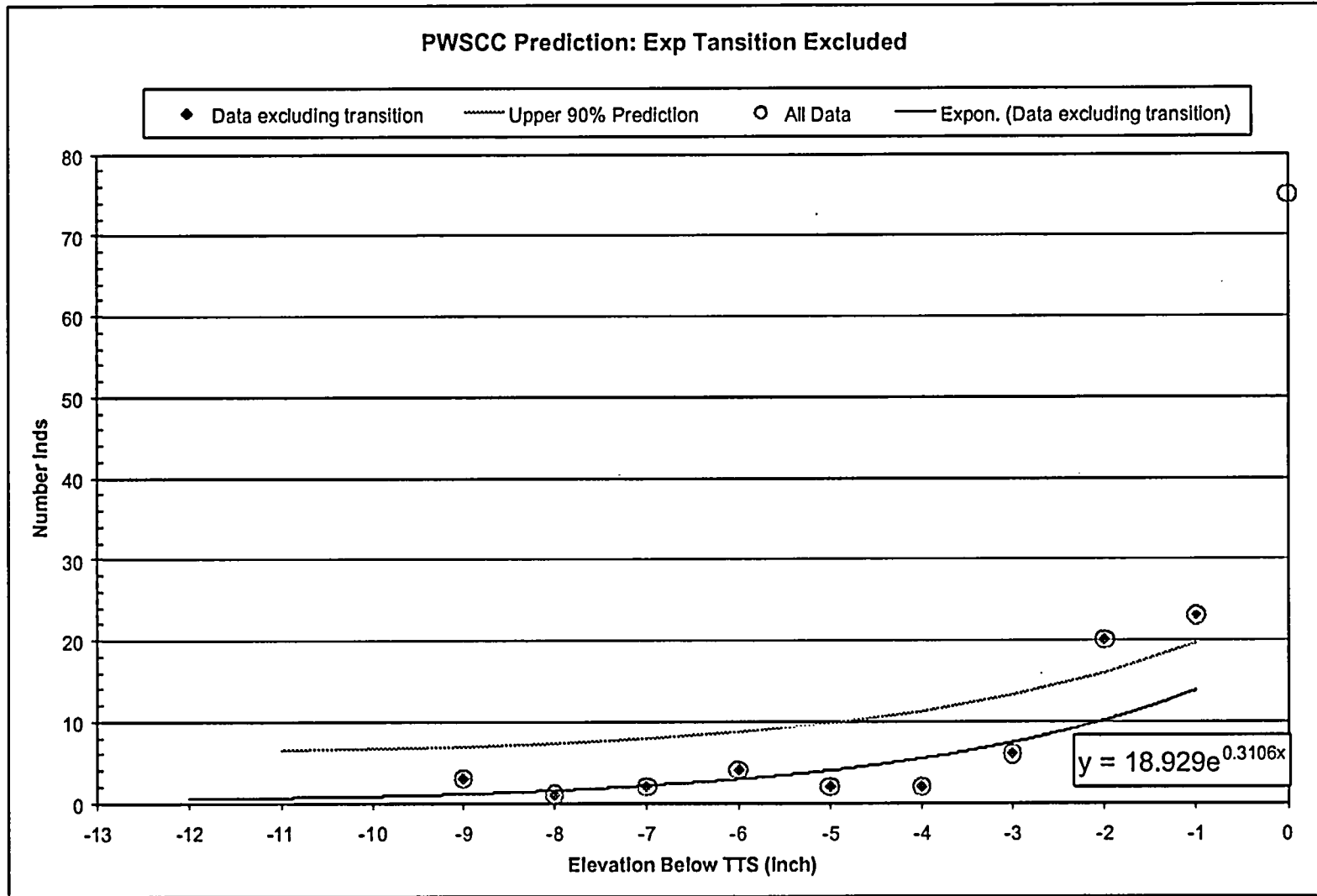


Figure 4.6

a,c,e



Figure 4.7

a,c,c



Figure 4.8

a,c,e



Figure 4.9



5.0 SEQUOYAH UNIT 2 RESPONSE TO PREVIOUS NRC RAIS

The NRC staff has previously transmitted further requests for additional information (RAIs) to utilities planning to implement the W* plugging criterion. The SQN2 responses to the previous RAIs that are applicable to a plugging criterion that utilizes a *non-degraded W* length (i.e., no service induced degradation is present)* are provided below. The responses have been grouped into three categories: inspection results summary, structural analysis related and steam line break leakage considerations.

5.1 INSPECTION RESULTS SUMMARY

5.1.1 Discussion of Inspection History at Sequoyah Unit 2 (Callaway RAI # 18 and # 23, St. Lucie Unit 2 RAI #26)

Table 5-1 presents a summary of the axial and circumferential PWSCC for the last five outages at SQN2.

Inspection	SG 1		SG 2		SG 3		SG 4	
	Axial	Circ	Axial	Circ	Axial	Circ	Axial	Circ
U2C8 (1997)	0	1	3	1	3	0	1	1
U2C9 (1998)	2	0	5	1	5	4	1	0
U2C10 (1999)	0	1	6	1	3	3	1	0
U2C11 (2001)	5	0	5	1	4	0	6	5
U2C12 (2003)	1	0	6	1	3	3	1	0
Total	8	2	25	5	18	10	10	6

Table 5-2 presents a summary of all historical PWSCC indications from the SQN2 EOC-8 through EOC-12 outages that includes elevation below TTS, flaw length, and flaw amplitude.

Table 5-2										
Unit	Cycle	S/G	Row	Col	Location	Elevation	NDE Indicated			
							Ax/Circ	Length		Max Volts
								Inches	Deg	
2	12	1	15	33	HTS	-8.67	AXIAL	0.69		2.94
2	12	2	11	60	HTS	-6.74	AXIAL	0.47		0.59
2	12	2	19	72	HTS	-0.79	AXIAL	0.17		0.35
2	12	2	20	60	HTS	-0.52	AXIAL	0.15		0.43
2	12	2	35	40	HTS	-6.75	AXIAL	0.10		0.33
2	12	2	35	40	HTS	-7.25	AXIAL	0.77		2.39
2	12	2	35	40	HTS	-7.96	AXIAL	0.09		0.49
2	12	3	21	30	HTS	-9.48	AXIAL	0.21		0.72
2	12	3	31	62	HTS	-0.5	AXIAL	0.12		0.33
2	12	3	35	31	HTS	-9.42	AXIAL	0.31		1.91
2	12	4	6	46	HTS	-0.68	AXIAL	0.10		0.51
2	11	1	2	9	HTS	-1.32	AXIAL	0.15		0.36
2	11	1	2	9	HTS	-0.5	AXIAL	0.15		0.41
2	11	1	2	9	HTS	-0.08	AXIAL	0.15		0.38
2	11	1	2	34	HTS	-0.85	AXIAL	0.24		0.28
2	11	1	19	39	HTS	-2.51	AXIAL	0.55		2.03
2	11	2	6	56	HTS	-0.6	AXIAL	0.16		0.4
2	11	2	7	24	HTS	-0.18	AXIAL	0.16		0.29
2	11	2	18	17	HTS	-3.17	AXIAL	0.12		0.52
2	11	2	22	60	HTS	-0.77	AXIAL	0.43		8.03
2	11	2	37	64	HTS	-6.22	AXIAL	0.21		0.56
2	11	3	1	54	HTS	-0.51	AXIAL	0.32		0.49
2	11	3	5	16	HTS	-5.26	AXIAL	0.17		0.33
2	11	3	12	2	HTS	-0.27	AXIAL	0.14		0.28
2	11	3	19	65	HTS	-2.98	AXIAL	0.28		1.94
2	11	4	2	37	HTS	-1.55	AXIAL	0.17		0.22
2	11	4	2	40	HTS	-1.03	AXIAL	0.11		0.62
2	11	4	11	26	HTS	-5.58	AXIAL	0.41		0.36
2	11	4	13	60	HTS	-4.49	AXIAL	0.11		0.46
2	11	4	15	8	HTS	-2.74	AXIAL	0.15		0.72
2	11	4	15	70	HTS	-4.19	AXIAL	0.23		2.44
2	10	2	2	59	HTS	-1.75	AXIAL	0.09		0.76
2	10	2	3	93	HTS	-0.85	AXIAL	0.23		0.60
2	10	2	7	63	HTS	-1.5	AXIAL	0.14		0.46
2	10	2	7	86	HTS	-0.43	AXIAL	0.16		0.53
2	10	2	13	72	HTS	-0.2	AXIAL	0.12		0.31
2	10	2	21	50	HTS	-0.18	AXIAL	0.15		0.63
2	10	3	7	7	HTS	-2.07	AXIAL	0.10		0.29
2	10	3	10	27	HTS	-0.84	AXIAL	0.21		0.39
2	10	3	19	46	HTS	-3.78	AXIAL	0.38		2.73
2	10	4	38	61	HTS	-2.62	AXIAL	0.14		0.50
2	9	1	36	33	HTS	-0.32	AXIAL	0.13		0.61
2	9	1	1	76	HTS	-0.31	AXIAL	0.14		0.41
2	9	2	2	20	HTS	-0.44	AXIAL	0.08		0.7
2	9	2	4	55	HTS	-0.66	AXIAL	0.10		0.91
2	9	2	8	55	HTS	-0.21	AXIAL	0.12		1.22
2	9	2	12	71	HTS	-0.1	AXIAL	0.08		0.64
2	9	2	22	76	HTS	-1.02	AXIAL	0.06		0.56
2	9	3	23	23	HTS	-0.14	AXIAL	0.23		0.82
2	9	3	31	33	HTS	-2.64	AXIAL	0.27		1.09
2	9	3	31	33	HTS	-2.35	AXIAL	0.29		0.51
2	9	3	31	33	HTS	-1.04	AXIAL	0.22		0.69
2	9	3	22	36	HTS	-0.21	AXIAL	0.12		0.7
2	9	4	12	64	HTS	-1.9	AXIAL	0.13		0.77
2	8	2	2	53	HTS	-0.55	AXIAL	0.16		1.48
2	8	2	10	54	HTS	-3.88	AXIAL	0.32		4.08
2	8	2	27	49	HTS	-1.34	AXIAL	0.11		0.91
2	8	3	22	12	HTS	-0.12	AXIAL	0.14		1.8
2	8	3	23	7	HTS	-0.43	AXIAL	0.18		1.59
2	8	3	24	67	HTS	-2.38	AXIAL	0.21		0.67
2	8	4	7	17	HTS	-0.15	AXIAL	0.32		3.55

Table 5-2 (cont'd)										
Unit	Cycle	S/G	Row	Col	Location	Elevation	NDE Indicated			
							Ax/Circ	Length		Max Volts
								Inches	Deg	
2	12	2	6	20	HTS	-0.02	CIRC		46	0.31
2	12	3	8	23	HTS	-0.03	CIRC		27	0.5
2	12	3	24	31	HTS	-0.22	CIRC		41	0.71
2	12	3	34	31	HTS	-9.8	CIRC		45	1.35
2	11	2	37	64	HTS	-6.41	CIRC		32	0.67
2	11	4	12	60	HTS	-0.36	CIRC		97	0.98
2	11	4	15	60	HTS	-3.59	CIRC		69	0.32
2	11	4	18	60	HTS	-3.55	CIRC		92	3.75
2	11	4	20	45	HTS	-3.64	CIRC		48	1.46
2	11	4	24	9	HTS	-2.67	CIRC		74	1.95
2	10	1	25	39	HTS	-1.52	Circ		31	0.8
2	10	2	19	82	HTS	-0.63	Circ		27	0.8
2	10	3	12	30	HTS	-0.17	Circ		30	0.35
2	10	3	12	36	HTS	-0.14	Circ		77	0.75
2	10	3	12	73	HTS	-0.01	Circ		30	0.2
2	9	2	8	77	HTS	-0.08	Circ		25	0.61
2	9	3	13	31	HTS	-0.09	Circ		32	0.2
2	9	3	12	40	HTS	-0.11	Circ		28	0.9
2	9	3	13	41	HTS	-0.2	Circ		39	0.85
2	9	3	19	25	HTS	-0.1	Circ		25	0.52
2	8	4	8	63	HTS	-1.84	Circ		67	2.09

5.1.2 Discussion of Industry Experience (Callaway RAI # 23 and # 65)

As noted above, a distribution of indications has been conservatively defined for the WEXTEX Region of the SQN2 steam generators. The potential occurrence of indications for Model 51 steam generators will be projected uniformly over the entire length of the joint in the SLB Leakage Model. This is based on the indications being potentially caused by tubesheet hole drilling anomalies during manufacture and the propensity for tube indications at tube hole surface anomalies in a previous Westinghouse laboratory program involving hydraulically expanded joints. It is assumed that potential corrosion of the WEXTEX tube joints would be similar because the anomalies would be sites of locally elevated residual stress. It is also based on the lack of indications in smooth bore, anomaly-free tube holes in hydraulically expanded joints (Alloy 600 tubes) in a laboratory program performed by Westinghouse for EPRI. This is conservative because based on observations at three hydraulic expansion (HE) joint plants of the Plant A tube size, most of the irregularities occurred in the upper reaches of the tubesheet. A more detailed set of data was received from one plant. Most of the signals recorded in the profilometry file were characterized as bulges. For the most part, the profilometry supports a declining trend of indications from the top of the tubesheet (see Section 4.0).

5.2 STRUCTURAL ANALYSIS

5.2.1 Determine Impact of Locked Tubes on W* (Diablo Canyon RAI # 1)

Locked tube residual axial loads occur because of packing and/or denting of the tube-to-tube support plate crevice while the plant is operating, i.e., when the tube is strained in the axial direction by primary-to-secondary pressure end cap load. Hence, the residual load in the tube is equal to the normal operating load. When the plant cools, a portion of the residual strain, and the attendant residual load remains. When the plant returns to power, the load at operating conditions is restored to the same level that was present when the locking occurred, i.e., at normal operating conditions. Since the TSP is restored to the elevation it occupied at the time of locking, it imparts no additional load on the tube. In other words, as the pressure load increases strain in the tube, the residual downward load of the tube on the TSP decreases. The W* criteria were developed to provide a margin of safety of three relative to the loads corresponding to normal operating conditions.

The second effect of the locked tube loading is the Poisson contraction of the tube in the hoop and thickness direction. Again, the axial stress conditions in the tube during operation are unaffected by locking of the tube at the TSP. The tensile test results used to demonstrate that the value used for the coefficient of friction were from conservative test programs. The equations used to calculate the coefficient of friction also did not account for the axial load, hence, the calculated values for the tests are lower than the actual values. Moreover, the configuration of the tensile tests also results in a Poisson contraction of the tube over the full range of the test load. This is conservative relative to demonstrating the factors of safety relative to the requirements of RG 1.121, e.g., testing to 3 times the required axial force results in a Poisson contraction three times that of the nominal condition.

In summary, implicitly ignoring the potential effects of the tube being locked at the TSPs is conservative to determining the W^* value. Even if a loss of engagement is postulated to be possible, and the effect of the locked condition is evaluated, the locked condition has no effect on the required W^* length. Therefore, the implicit assumption that the tubes are not locked at the TSP is either conservative or not significant to the determination of W^* (Reference 5.1).

5.2.2 Impact of Tubesheet Bow on Pullout and Leak Rate Testing (St. Lucie 2 RAI # 8, Callaway RAI # 8 and #55)

Tubesheet bow is the flexing of the tubesheet in response to the primary-to-secondary side pressure difference results in a dilation of the holes above the mid-plane of the tubesheet during normal operation and postulated faulted conditions. The contact pressure decreases above and increases below the approximate mid-plane² of the tubesheet. The dilation does not have to be simulated since it can be treated analytically using the Theory of Elasticity.

In situ leak rate tests are conducted at ambient conditions and there is no differential pressure across the tubesheet. Thus, there are two conditions that are atypical of normal operating and postulated accident conditions. In summary, the increase in temperature tends to make the joint tighter, and the increase in differential pressure across the tubesheet will tend to make the joint looser. In addition, for structural integrity testing, the increase in pressure internal to the tube will act to tighten the joint and increase the strength of the joint. Thus, the act of testing may bias the results in a non-conservative manner at the elevation of the degradation being tested. It is noted that there is no hole dilation at the location of the neutral plane of the tubesheet, slightly below mid-plane, and such testing which results in no leakage is indicative of operating and accident condition results to be expected at lower elevations within the tubesheet.

In situ structural testing is not likely to be meaningful in demonstrating compliance with performance criteria, i.e., demonstrating a resistance to pullout of greater than three times the normal operating pressure differential. Moreover, the difference in contact pressure during in situ testing means that the leak rate data cannot be used directly to quantify potential leak rates. This does not mean that an analytical procedure could not be developed to deal with such quantification, that is the basis for correlating the leak rate to the inverse of the loss coefficient and further correlating the loss coefficient to the tube-to-tubesheet contact pressure.

The effect of tubesheet bow can result in an average decrease in the contact pressure during postulated accident condition for the Model 51 tubes. For the tubes tested to date, in situ testing resulted in no measurable leakage. However, the contact pressure during the performance of the in situ test was significantly less than the contact pressure present when the laboratory tests were performed, almost all of which leaked. Thus the leak rate tests performed in situ are relevant to demonstrating whether or not an indication leaks. Although the leak rate from a leaking indication may not lend itself to a precise quantified prediction of the leak rate during operation, it can be used to estimate whether or not the leak rate would be significant during operation or postulated accident conditions. A deformation balance can be performed to

² The location of the neutral plane of the tubesheet is slightly below the mid-plane because of the membrane stress caused by the distributed pressure load.

determine if lower pressure test should be performed (results from an analysis of Model F SGs were that higher pressure led to higher leakage).

During the Fall 2003 inspection at a plant with CE steam generators, a 1.9 V (by + Point), 140° arc length, 99% through wall (by phase angle) circumferential crack (PWSCC) at the top of the tubesheet was in situ tested with no leakage being reported at the postulated SLB pressure difference.

5.2.3 Tube Pull Out Testing Description (Callaway RAI # 25)

The pullout testing program and results are described in the "Pullout Test Specimen Descriptions" section of WCAP-14797, Rev. 2, Section 4.2.2, and is summarized below.

The W* pullout test samples were selected from a number of specimens prepared in the W* program to provide a lower bounding case condition with regard to pullout resistance. The W* pullout samples consisted of carbon steel collars approximately 4 inches in length, 2.25 inches in outside diameter and 0.890 inch in inside diameter. Expanded into each collar by the WEXTEX process was mill annealed Alloy 600 (ASME SB-163) steam generator tubing section approximately 12 inches in length. The tube yield strength was 58 ksi. The nominal unexpanded outside diameter of the tube was 0.875 inches.

Since the WEXTEX expansion is a high energy process which causes the tube OD to impact and to be deformed into even small variations in the tubesheet hole bore surface, the feature which is of most significance is the surface finish of the tubesheet hole. The Series 51 SG tubesheet hole requirement was 250 microinch rms maximum. The samples in the test program were procured to a 100 to 250 rms requirement. For the W* pullout tests, two tubesheet collar specimens were selected, one specimen which appeared to have a bore surface roughness at the upper end of the bare finish requirements, and one with a smooth. Both of tubesheet collar specimens had uniform diameter profiles.

The collars used to simulate the tubesheet were fabricated from 1018 cold rolled carbon steel round bars with mechanical properties similar to that of the tubesheet material. The collar inside diameter was selected to match these size holes in the Model 51 tubesheet and the outside diameter was selected to provide the same radial stiffness as the tubesheet hole.

The WEXTEX samples fabricated for pull force testing were of a double ended configuration. After WEXTEX expansion, the samples were qualitatively checked for joint leak tightness. About 70% of the specimens exhibited a slight degree of looseness in the hoop direction in that it was possible to rotate the tube by an estimated 1 or 2 degrees ($1^\circ \approx 7$ mils on the tube OD).

The samples were also noted to have [

]b,c,e

5.2.4 Tubesheet Finite Element Model Discussion (Callaway RAI # 27 and # 43)

Loads are imposed on the tube as a result of tubesheet bowing under various pressure and temperature conditions. The finite element analysis of the tubesheet, channelhead, and lower shell were performed to determine the unit displacements throughout the tubesheet for two pressure unit loads (primary and secondary side) and three thermal unit loads (tubesheet, shell, and channel head). The analysis yielded the unit displacements throughout the tubesheet for these five unit loads. The normal operating and faulted conditions (pressure and temperature) were then applied to these unit displacements for calculating the tube-to-tubesheet contact pressure distribution from the top to the bottom of the tubesheet.

The pressure and temperature parameters for the feedline break, steam line break, and loss of coolant accident (LOCA) events were from a generic accident analysis. It is shown in Section 3.0 of this report that the generic temperature and pressure parameters used in the structural analysis bound the values used in the accident analysis of the SQN2 steam generators.

5.2.5 Ligament Tearing Discussion (Callaway RAI # 30)

One of the concerns that must be addressed in dealing with cracks in SG tubes is the potential for cracked tube radial ligament tearing to occur during a postulated accident when the differential pressure is significantly greater than during normal operation. While this is accounted for in the strength evaluations that demonstrate a resistance to pullout in excess of $3 \cdot \Delta P$ for normal operation and $1.4 \cdot \Delta P$ for postulated accident conditions, the potential for ligament tearing to significantly affect the SLB leak rate predictions needs to be accounted for.

Ligament tearing considerations for circumferential tube cracks that are located below the W^* depths within the tubesheet are significantly different from those for potential cracks at other locations. The reason for this is that W^* has been determined using a factor of safety of three relative to the normal operating pressure differential and 1.4 relative to the most severe accident condition pressure differential. Therefore, the internal pressure end cap loads which normally lead to an axial stress in the tube are not transmitted below about $1/3$ of the W^* depth. This means that the only source of stress acting to extend the crack is the primary pressure acting on the flanks of the crack. Since the tube is captured within the tubesheet, there are additional forces acting to resist opening of the crack. The contact pressure between the tube and tubesheet results in a friction induced shear stress acting opposite to the direction of crack opening, and the pressure on the flanks is compressive on the material adjacent to the plane of the crack, hence a Poisson's ratio radial expansion of the tube material in the immediate vicinity of the crack plane is induced which also acts to restrain the opening of the crack by increasing the contact pressure between the tube and the tubesheet. In addition, the differential thermal expansion of the tube is greater than that of the carbon steel tubesheet, thereby inducing a compressive stress in the tube below the W^* length.

A scoping evaluation of the above effects was performed by ignoring the forces that resist the crack opening, and simply looking at the effect of the pressure acting to open the crack. If a 360° throughwall crack is considered, the stress from the pressure on the flanks is 0.206 or 20.64% of the stress that would result from an end cap pressure load for the same pressure. The primary pressure during normal operation and during a postulated accident is 2250 and 2665 psia respectively. The actual pressure difference between accident and normal operating conditions is 415 psi or 18% and the relative effect is equivalent to a change in pressure of 100 psi or 4% if the source of the stress were the end cap pressure differential.

The magnitude of the effect can also be used to conservatively estimate the ligament thickness of tube material affected. Using the ASME Code specified minimum yield stress of 35.2 ksi at 650°F, the applied forces can be calculated as if the pressures were applied to the entire cross-sectional area of the tube material, thus representing the maximum force that can be applied to the tube as the result of a pressure on the crack flanks. These calculated maximum forces are 290.9 and 349.6 lbs at internal pressures of 2250 and 2665 psia respectively. So as not to exceed the yield stress, less than 9% of the cross-sectional area of the tube is required to resist the maximum force of 344.6 during a postulated accident. This equates to a circumferential crack that extends 360° and is 92% through-wall, i.e., the remaining material is less than 3.5 mils thick. The corresponding value for the normal operating condition is a little more than 3.0 mils. Thus, the difference in required wall thickness between the normal operation and accident condition pressures is on the order of 0.5 mil. If the resisting forces discussed above were to be included in this evaluation, the difference would be significantly less.

In summary, considering the worst-case scenario, the likelihood of ligament tearing from radial circumferential cracks resulting from an accident pressure increase is small since at most, only 8% of the cross-sectional area is needed to maintain tube integrity. Also, since the crack face area will be less than the total cross-sectional area used above, the difference in the force applied as a result of normal operating and accident condition pressures will be less than the 53.7 lbs calculated for the Model 51 steam generators. Therefore, the potential for ligament tearing is considered to be a secondary effect of essentially negligible probability and should not affect the results and conclusions reported for the W* evaluation. The leak rate model does not include provisions for predicting ligament tearing and subsequent leakage, and increasing the complexity of the model to attempt to account for ligament tearing has been demonstrated to be not necessary (Reference 5.2).

5.2.6 Discuss No Contact Length for Normal/Postulated Accident Conditions

The no contact length for each of the SG zones for both normal and postulated accident conditions is the axial length over which dilation of the tubesheet causes the mechanical interference fit contact pressure between the tube OD and the tubesheet hole surface to reduce to zero. The no contact length during normal operating conditions is less than 1.0 inch in Zones A and B. The no contact length during a postulated SLB is less than 3 inches in Zones A and B.

All WEXTEx expansions are assumed to have a small gap over the upper 0.7 inches of distance below the BWT for both pullout force and leakage analyses.

5.3 STEAM LINE BREAK LEAKAGE CONSIDERATIONS (CALLAWAY RAI # 59)

The leak rate model included in Reference 2.1 is based on data from crevice tests and from cracked tube tests. The computer code CRACKFLO is based on the theory of two phase flow and crack opening area. Crevice flow uses a theory model with empirical data for validation at various levels of contact. An empirical effective axial crack length is used. The individual elements of which have been validated against test data. The DENTFLO model is based on a crack in series with the crevice. The model balances flow through the crack and through the crevice such that the continuity is maintained. The pressure at the exit of the crack must match the pressure at the entrance to the crevice. A deterministic corrosion calculation algorithm has been demonstrated to be conservative to a Monte Carlo simulation of uncertainties.

5.3.1 Validation of W* Leak Rate Model Through In Situ Testing (Callaway RAI # 63, St. Lucie 2 RAI # 19)

The following discussion is included for information only. The use of a bounding leak rate model based on test data for the SQN2 SG indications obviates the need to apply the standard W* leak rate model.

W* Leakage Model and In Situ Testing Validation Program

The W* leakage model was developed based upon first principles of leakage from a crack in a tight crevice. Leakage from a tight crevice is a series path through the crack with the crack opening constrained by the tubesheet, and followed by leakage through the tight crevice. In the leakage model, the total steam line break (SLB) pressure drop occurs from the tube inside diameter (ID) to near the top of the tubesheet (TTS) at the bottom of the WEXTEx transition (BWT). The crack inside the tubesheet, with very small clearances, cannot open significantly due to the constraint of the tubesheet hole ID. Leakage tests were performed to directly model this effect by measuring the leakage at the upper tip of the crack with small tube to tubesheet clearances. The leak rates for the constrained crack are correlated with contact pressure using an equivalent CRACKFLO crack length to represent leakage. Since the equivalent crack length is the length that gives the measured leak rate, the plot of Figure 6.4-1 of WCAP-14797, Revision 2, is essentially the leak rate through the crack at the crack tip versus contact pressure. The principal purpose in introducing the CRACKFLO equivalent length, rather than measured leakage, is to permit adjustments of the measured leak rates for the pressure drop across the crack in series with the crevice pressure drop for the leakage model.

The test data for leakage through the crevice is modeled using the crevice loss coefficient correlated with contact pressure. The loss coefficient is fit to each measured leak rate for the correlation with contact pressure, such that the correlation is essentially the leak rate through the crevice versus contact pressure. The use of a loss coefficient correlation, rather than leak rate, permits adjustments of the leak rate for the pressure drop across the crevice in series with the crack pressure drop.

Both the effective crack length and loss coefficient correlations are obtained as regression fits from the leak rate measurements. These values, therefore, are not analytical results. The

analytical model is only used to perform the series leakage analysis, and consists primarily of adjustments to obtain equal leakage through the crack and crevice for the total tube ID to crevice exit pressure drop. This is a first principles fluid flow calculation based on prototypic, experimentally developed, effective lengths and loss coefficients. Combined crack and crevice leak tests by in situ testing were been performed in 2R9 and 2R10 as described below.

To date, 14 W* indications have been in situ leak tested in the industry: 7 at Diablo Canyon Unit 2 (DCPP 2) at refueling outages 2R9 (1999) and 2R10 (2001), 1 at Sequoyah Unit 2 (SQN 2), and 6 at Beaver Valley Unit 1 (BVPS 1). The indications are listed in Table 5-3. No leakage was observed in any test. Most of the indications were located near the bottom of WEXTX transition (BWT), such that the tubesheet provided minimal crevice restriction. The DCPP 2 indications are located in tubes that had been unplugged, were tested to normal operating pressure differential, and were returned to service. Non-deplugged W* indications at DCPP have not grown deep enough to satisfy the requirements for leak testing.

It is the TVA intent to only in situ test indications that meet the requirements of the EPRI In Situ Guidelines.

**Table 5-3
Industry In Situ Test Results for Axial PWSCC in WEXTEX Region**

Plant	Year	SG	Tube	Deplug tube	Crack distance below BWT, (below TTS for SQN and BVPS), inch	Peak Volt	Crack Length inch	Max Depth	Approx Length > 80%, inch	Test Pressure	Leak Rate
DCPP 2	1999	1	R3C59	Yes	0.51	5.6	0.27	100%	0.23	NOP	0
DCPP 2	1999	1	R7C62	Yes	0.59	4.2	0.35	80%	None	NOP	0
DCPP 2	1999	2	R31C25	Yes	0.98	4.0	0.24	70%	None	NOP	0
DCPP 2	2001	3	R7C52	Yes	0.56	3.4	0.43	94%	0.37	NOP	0
DCPP 2	2001	4	R3C5	Yes	0.55	1.5	0.83	100%	0.63	NOP	0
DCPP 2	2001	4	R2C29	Yes	3.52	4.5	0.91	100%	0.84	NOP	0
DCPP 2	2001	4	R2C29	Yes	1.83	0.9	0.34	100%	0.1	NOP	0
SQN 2	1997	4	R7C17	No	0.15	3.6	0.32	100%	0.02	3dpNO	0
BVPS 1	1997	A	R10C51	No	0.24	0.7	0.30	77%	None	3dpNO	0
BVPS 1	1997	A	R27C28	No	3.20	1.2	0.22	35%	None	3dpNO	0
BVPS 1	1997	B	R5C83	No	0.35	1.5	0.21	30%	None	3dpNO	0
BVPS 1	1997	C	R27C31	No	0.60	0.9	0.18	44%	None	3dpNO	(1)
BVPS 1	2001	A	R7 C59	No	1.86	1.98	----	33%	N/A	SLB ?P	0
BVPS 1	2001	B	R35C22	No	1.51	1.3	----	50%	N/A	SLB ?P	0

⁽¹⁾ In situ pressure testing tooling system leakage. No leakage judged to be due to a flaw.

W* in situ leak tests are conducted at the normal operation differential pressure. If the indication leaks, the test will be continued up to the SLB differential pressure, and the tube will be repaired. If leakage is not detected at the normal operation pressure difference, the test would be terminated without extending the pressure differential to SLB conditions. All tubes that are tested *in situ* are removed from service regardless of the test results.

Also, it is noted that in situ leak testing of likely throughwall indications near the top of the tubesheet does provide meaningful information relative to the potential for throughwall indications located deeper in the tubesheet to leak. The in situ testing experience has been such that indications do not leak. Because the hole dilation diminishes with distance into the tubesheet, there is a location with a post accident condition radial contact load that corresponds to that achieved during the in situ testing. Thus, testing of through wall indications near the top of the tubesheet supports the evaluations that conclude that leakage from tube indications deeper in the tubesheet would be negligible.

5.3.2 Discussion of Tube Radial Contraction Effect (Diablo Canyon RAI # 2)

Equations 4.4-4 and 4.4-7 of WCAP-14797-P, Rev. 2, do not include a term to account for a contraction of the tube by the Poisson effect due to tube end loading. Had this been accounted for, the term

$$\frac{P_i}{E_t} \left[\frac{2a^2b}{b^2 - a^2} \right] \quad \text{(Current 4.4-4 Term)}$$

in both equations 4.4-4 and 4.4-7 would have been written as

$$\text{Corrected Equation} \quad \frac{P_i}{E_t} \left[\frac{(2-\nu)a^2b}{b^2 - a^2} \right] \quad \text{(Modified 4.4-4 Term)}$$

The net result of including the Poisson effect in the expression for the outward movement of the tube OD due to internal pressurization, i.e., accounting for the end cap load on the tube, would be a maximum 15% reduction in the calculated value for the outward movement of the tube OD due to internal pressure. This is based on a value of Poisson's ratio, ν , of 0.3 so $2-\nu$ or 1.7 should have been used instead of 2 as the constant in the numerator. Calculations have been performed to determine the net result of including the aforementioned Poisson effect in the expression for the tube-to-tubesheet contact pressure, with equation 4.4-7 written as:

$$P = \frac{\frac{P_i}{E_t} \left[\frac{(2-\nu)a^2b}{b^2 - a^2} \right] + b(a_{tbe} - a_{TS})(T - 70)}{\frac{b}{E_{TS}} \left[\frac{c^2 + b^2}{c^2 - b^2} + \nu \right] + \frac{b}{E_t} \left[\frac{b^2 + a^2}{b^2 - a^2} - \nu \right]} \quad \text{(Modified 4.4-7)}$$

For the range of contact pressures associated with the data in Figure 6.4-2 of WCAP-14797, Rev. 2, including the Poisson effect due to the tube end cap load produces net reductions in the contact pressure ranging from 50-350 psi, depending on the magnitude of the contact pressure plotted (which is a function of the internal pressure in the leak test specimen. A slight reduction of 50-100 psi occurs in the contact pressure for data points on the lower end of Figure 6.4-2, when accounting for the Poisson effect, thus shifting the data points slightly to the left. For the highest data points of Figure 6.4-2, a contact pressure reduction on the order of 250-350 psi would be calculated to occur, shifting these data points farther to the left. Hence, overestimation of the contact pressure through not accounting for the contraction of the tube due to the end cap load causes the scale on the crevice resistance correlation of Figure 6.4-2 and the effective crack length correlation of Figure 6.3-8 of WCAP-14797, Rev. 2 to shift outward. Modifications to account for the Poisson effect will cause both curves to become steeper, resulting in higher crevice resistance and a smaller effective crack length for a given calculated contact pressure. Hence, neglecting the Poisson effect in calculating the contact pressure for the test specimens produced conservative values of effective crack length and loss coefficient for the given contact pressures. This effect, however, is neutralized in the application of these correlations because lower contact pressures will be applicable for applying the correlations to calculate leak rates as described in Section 6.4 of WCAP-14797, Rev. 2. That is, the same contact pressure formula used to develop the leak rate correlations is also used to apply the correlations for calculating leak rates in Section 6.4. Hence, calculated leak rates using contact pressures which account for the Poisson effect would be expected to be negligibly different (estimated as less than a few

percent) from those calculated neglecting the contraction of the tube due to the end cap load. The conclusions from the leak rate analysis would not be affected by the absence or presence of the Poisson's term in the calculation of the contact pressure.

In retrospect, it would have been more appropriate to include the Poisson contraction effect in the analyses. However, the expected negligible impact does not justify performing a complete reanalysis of the data with the Poisson effect included (Reference 5.3). Moreover, it is noted that because the load transmitted along the tube diminishes with depth into the tubesheet, the original equation is correct below what would be a W^* distance without the application of a safety factor to the end cap load. This would further diminish any effect below that distance and further support the conclusion that a correction, really a modification, to the analysis is not necessary.

5.3.3 Discussion of Secondary to Primary Leakage Following Postulated LOCA (Diablo Canyon RAI # 3)

During normal operation, the tube-to-tubesheet contact pressure in the region above the tubesheet neutral bending axis is reduced by upward bending of the tubesheet due to the primary-to-secondary ΔP . This reduction in contact pressure is a function of elevation and radial location from the center of the tubesheet, and is accounted for in the determination of the W^* lengths. During a postulated LOCA event, the primary side pressure drops to atmospheric conditions while the secondary side remains at 1005 psia. The component of the tube-to-tubesheet contact pressure resulting from primary pressure inside the tube is lost, and the external pressure on the tube acts to further reduce the tube-to-tubesheet contact pressure. However, the reversal of the ΔP across the tubesheet causes the tubesheet to bow downward, providing an increase in that component of the tube-to-tubesheet contact pressure above the neutral axis of the tubesheet. In the top four inches of the W^* region near the top of the tubesheet, the increase in contact pressure due to downward tubesheet bending more than offsets the reduction in contact pressure due to the reversed ΔP across the tube wall. For instance, at a distance of 2" below the TTS, the tube-to-tubesheet contact pressure resulting from the primary-to-secondary ΔP is 790 psi during normal operation, while the maximum loss of contact pressure due to tubesheet bending is 1549.5 psi; the net minimum contact pressure (including an additional 509.8 psi contact pressure due to thermal expansion and 693 psi due to the residual WEXTEx contact pressure) is 443.3 psi. For postulated LOCA conditions, the loss of primary side pressure in conjunction with a secondary side pressure of 1005 psi results in a calculated contact pressure due to the secondary-to-primary ΔP of -1225.6 psi. However, tubesheet bow in the opposite direction adds 970.6 psi in addition to the 509.8 psi contact pressure due to thermal expansion and 693 psi from the WEXTEx expansion residual preload; the net minimum contact pressure is 947.8 psi, which is 504.5 psi greater than the contact pressure during normal operating conditions. The net effect is a tighter joint at the top of the tubesheet during a postulated LOCA event than exists during normal operating conditions. Past analyses performed by Westinghouse have shown that secondary-to-primary in-leakage through free span cracks occurs at a slower rate than primary-to-secondary leakage at the same ΔP . Based on this experience, along with the lower magnitude of the LOCA ΔP relative to that during normal operation, and with the increase of tube-to-tubesheet contact pressure at the TTS caused by the reverse tubesheet bow, in-leakage to the primary side during a LOCA event would be expected to occur at a slower rate than primary-to-secondary leakage during normal operation, which is limited to 150 gpd (0.1 gpm). In-leakage to

the primary side through W* tubes during a LOCA event is therefore assured of occurring at a slower rate than 0.1 gpm and would therefore not affect the plant LOCA analyses (Reference 5.3).

5.3.4 Discussion of Consistency of Leak Rate Results – C* Test Data Applicability

5.3.4.1 Introduction

Reference 5.4 describes the development of criteria, designated W* (W-star), developed for utilities to use to disposition steam generator (SG) tube degradation when such degradation is found in the tube length that is within the tubesheet for tubes explosively expanded into the tubesheet, i.e., Westinghouse SGs with WEXTEX tube-to-tubesheet joints. A presentation was given to the NRC staff in 1996, Reference 5.5, and again in September 2003, Reference 5.6, further explaining the basis for the establishment of the criteria and its implementation.

Following the development of the W* criteria, two additional criteria were developed, designated H* for dealing with indications in tubes hydraulically expanded into the tubesheet in Westinghouse SGs and C* for dealing with indications in tubes explosively expanded, *explanded*, into the tubesheet in Combustion Engineering (CE) fabricated SGs. The information developed from these programs has been used to technically justify limiting the length of eddy current test (ECT) rotating pancake coil (RPC) inspection of the tubes within the tubesheet, notwithstanding the full length inspection using bobbin coil technology. The rationale is that the regulatory criteria relative to margin against burst during normal operation and postulated steam line break (SLB) events is precluded by the presence of the tubesheet and that the total leak rate from all indications within the tubesheet would be less than the UFSAR accident analysis assumption for primary-to-secondary leakage in the faulted loop during a postulated SLB, typically less than 1.0 gpm. The only possible mode of burst for tubes with degradation within the tubesheet is expulsion from the tubesheet of a severed tube end. It has been found that the length of engagement required to preclude burst relative to the length required to meet leakage requirements is a function of the joint fabrication process. The length required to meet leak rate requirements is usually longer than the length required to prevent burst for explosively and hydraulically expanded joints. The number of circumferential indications in WEXTEX tube-to-tubesheet joints is very small, and the testing program demonstrated that axial indications would be expected to exhibit no or miniscule leak below the W* distance, hence the conclusion was expressed that degradation of any extent could be tolerated below W*.

Recent leak rate results obtained from a second series of tests of explanded joints were preliminarily found to be potentially significantly greater than those obtained from the first series of tests. This prompted one utility with CE designed SGs to conservatively increase the length of the RPC inspection within the tubesheet because the final analysis of the test data was, and still is, incomplete, hence the final results of the analysis for CE expansion joints were and are unknown. However, a thorough review has since confirmed the validity of the original testing (Reference 5.7). Several of the steps taken by the test operators effectively deoxygenated the deionized water that was used in the W* leak tests. Nitrogen sparging, dissolved oxygen measurements or frequent venting during heatup was adequate to remove oxygen from the test water. Cooldown procedures and between test machining steps were conducted in a manner such

that the sample was not exposed to air while at an elevated temperature. Therefore, it is highly unlikely that oxides formed within the tight annulus between the tube and the tubesheet stimulant that would have affected the leak rate results.

5.3.4.2 Testing Information

There have been several series of tests performed on specimens expanded into tubesheet simulating collars using installation techniques typical of those used to fabricate the original SGs. The results of these tests have led to the establishment of plugging or inspection criteria designated as W^* for WEXTEX, H^* for hydraulic, and C^* for Combustion Engineering tube-to-tubesheet joints. The predecessor criteria were F^* for force and L^* for leak rate from hard rolled tube-to-tubesheet joints. The F^* criterion involved no leakage from the tubesheet crevice and is of no interest in this discussion except to note that F^* was the length of engagement necessary to resist pullout of the tube from the tubesheet under all operating condition loads. The L^* criteria, the length of engagement to prevent leakage, was similar to the W^* criteria and the philosophy of development was the same. Because the length of engagement to prevent leakage, L^* , in hard rolled joints was so short, shorter than the F^* length, there was no consideration of allowing cracks to remain in service within the L^* length.

5.3.4.2.1 W^* Testing

The leakage from cracks inside the tubesheet is comprised of two leak paths. One path is the tube to tubesheet crevice above the top of the crack. The second leak path is related to the ability of a crack to open inside the tubesheet where the tubesheet constrains opening of the crack flanks in the radial and hoop directions. The W^* leak tests included two series of tests to separately measure leakage from the two leakage paths. The two tasks supported a W^* leak rate calculation model incorporating the two leakage paths in series and satisfying conservation of mass and momentum relations.

The leakage path for the tube-to-tubesheet crevice leakage was achieved by drilling holes through the collar simulating the tubesheet and tube. The area of the drilled holes in the tube was sufficient for the tests to approximate leakage from a tube severed at the area of the holes. In particular, some of the tubes were staked, i.e., deformed inward, at the holes to assure separation of the tube from the collar, effectively opening the leak path at the interface. The measured leakage from these tests represents crevice restriction as a function of tube to tubesheet contact pressure as the only limitation on leakage.

The second series of tests were performed as constrained axial crack leak tests. These tests were performed to reflect the limited ability of the crack to open inside the tubesheet as a reduction in leakage compared to a freespan crack or a severed tube. Tube sections were prepared with fatigue cracks, which conservatively model primary water stress corrosion cracks (PWSCC) since the fatigue cracks are uniformly throughwall with no ligaments and have a smoother crack face surface (less tortuosity) than corrosion cracks. The tubesheet collars were drilled with tight tolerances and the test tubes were ground on the OD in order to obtain small, well defined initial gaps to improve the accuracy of the contact pressure analyses. The collars were machined with a 360° groove with axial grooves to the top of the collar providing a large leakage path from the

circumferential groove to the top of the collar. For the leak tests, the upper tip of the fatigue crack was located at the bottom of the circumferential groove in the collar to provide a leak path from the crack tip to the top of the collar with a negligibly small resistance. These tests measure only the constraining effect of the tubesheet on crack opening and leakage to the tip of the crack. Tests were performed in two collars with initial ambient condition diametral tube-to-collar gaps of 0.4 and 0.9 mils to obtain variability in the contact pressures. The elevated temperature tests were performed with borated and lithiated water to simulate primary water conditions. These tests thus measured leakage from a constrained crack to the tip of the crack as a function of contact pressure. These test results in combination with the crevice leakage test results provide test data for the entire leakage path in support of the leakage model for tubesheet crack leakage.

The results from the crevice tests were used to develop a flow loss coefficient or resistance as a function of contact pressure between the tube and the tubesheet. This was necessary because the tubesheet bows upward during operation resulting in a varying contact pressure that is a minimum at the top of the tubesheet and a maximum at the bottom. The leak rate equation is,

$$Q = \frac{1}{\mu K} \frac{dP}{dx} \quad (1)$$

where Q is the leak rate, μ is the effective viscosity of the fluid (water or steam or a combination), K is the loss coefficient, and dP/dx is the axial primary-to-secondary pressure drop driving the fluid through the crevice. The test programs are conducted to solve the rearranged equation,

$$K = \frac{1}{\mu Q} \frac{dP}{dx}, \quad (2)$$

and results in the determination of the logarithm of K as a linear function of the contact pressure, P_c , between the tube and the tubesheet, see Figure 5.1. Three-dimensional finite element analysis was performed to map the tube-to-tubesheet contact pressure as a function of depth into the tubesheet at various radii from the center of the SG. This later step was taken to account for the dilation of the TS holes because the TS bows upward due to the primary-to-secondary pressure difference. In summary, a prediction of the potential leak rate from any and all indications within the tubesheet could be made based on a knowledge of the flaw distance below the top of the tubesheet, the temperature within the tubesheet, the radial location of the tube hole in the tubesheet (by row and column) and the primary-to-secondary operating conditions. The second series of tests was performed to measure the effect of the tubesheet on the leak rate from axial cracks in the SG tubes. The results of the analysis of the test data demonstrated that the loss coefficient would be extremely large for indications located below about 6 inches into the tubesheet.

The crevice testing was conducted at ambient and elevated temperature conditions using deionized (DI) water, and, based on Reference 5.7, also deoxygenated water. A review of the test data the test equipment and test conduct indicates no apparent anomalies and no reason to question the efficacy of the obtained data. A total of four specimens were tested at a variety of internal pressure and temperature conditions. The results of the tests exhibited similar trends with no single specimen dominating the results. Moreover, the room temperature test results

were consistent with the elevated temperature results according to the model, i.e., the major contributor to the leak rate behavior should be the viscosity for the same contact pressure conditions. Finally, a review of the testing program information from the time, including a meeting with the test engineer (now retired), indicates that the level of oxygen in the test water was minimized, a heated reservoir was used and the reservoir was vented periodically to control the pressure and remove oxygen.

5.3.4.2.2 H* Testing Programs

The initial H* tests were conducted in the late 1990's using Westinghouse Model F tube specimens hydraulically expanded into carbon steel collars to simulate the tube-to-tubesheet joint. The justification of the H* length also made use of test results documented in a 1988 Westinghouse report relative to demonstrating the efficacy of the hydraulically expanded joints in Model F SGs. Tests were conducted for two different lengths of engagement and a variety of induced contact pressures between the tube and the tubesheet. The contact pressure can be controlled by the internal pressure in the tube and the temperature at which the test is performed. The Model F SG tests were conducted using DI water at ambient and elevated temperatures and at various primary-to-secondary differential pressures simulating normal operation and postulated accident conditions. The analysis approach was the same as that for W* in that a loss coefficient as a function of contact pressure was calculated and used to predict the leak rate of potentially throughwall tube indications within the tubesheet. A review conducted in 2001 of the earlier test data indicated that the leak rate resistance could be a function of the time-at-temperature of the specimen, i.e., the leak rate may decrease with operating time.

It was postulated at the time by Westinghouse that the interaction of the hot deionized, but not deoxygenated, water could have resulted in oxidation of the tubesheet in the crevice leading to the decrease in the leak rate as a function of time. It was also postulated that a similar corrosive reaction would take place in primary water as the carbon steel would interact with boron carried through the crack. Replenishment of the boron would not take place once the flow was stopped and further corrosion would not take place. Thus, the test results would be expected to be in concert with field data wherein an operating plant with Model F SGs with hydraulically expanded tubes was concluded to have a tube that was severed or nearly severed several inches into the tubesheet without attendant leakage during operation or during in situ testing. A second laboratory testing program was undertaken using tube specimens representative of Westinghouse Model D5 SGs to extend the H* results to another class (different tube size) of Westinghouse SGs with hydraulically expanded tubes. Deoxygenated primary water was used as the testing medium for the second series of tests. The results from the tests indicated a slight, but not statistically significant, decrease in the leak rate as a function of joint length and/or contact pressure. In other words, the resistance to leaking primary water increased relative to the use of DI water. This information provided direct confirmation relative to the adequacy of the use of DI water for the H* crevice leak rate testing and probably the W* test program, both of which were conducted at the Westinghouse laboratory in Churchill, Pennsylvania. Subsequent information, Reference 5.7, indicates that the deionized test water would have been depleted of oxygen also.

5.3.4.2.3 C* Testing Programs

The approach taken to demonstrating compliance was to determine the depth within the tubesheet that degradation of any extent could be postulated for all of the tubes in the SG and the leak rate requirement of the UFSAR accident analyses leak rate assumption in the faulted loop during a postulated SLB event would not be exceeded. The required length of engagement was determined from a series of tests performed for the Combustion Engineering Owners Group (CEOG). A length of engagement on the order of 7 inches, including measurement error, was calculated to be sufficient to meet a typical leak rate requirement of 0.1 gpm, apportioned to the tube circumferential indications within the tubesheet, during a postulated SLB event if all of the tubes were considered to have 360° by 100% deep circumferential cracks at that elevation. The tests were conducted using typical tube sizes for CE designed plants, test blocks and collars representative of the tubesheet fabrication process, and also included a tubed section of tubesheet from a plant that was cancelled during fabrication of the components. The expansion installation process for the tubes into the tubesheet holes was either duplicated or the tube-to-tubesheet joints already existed. Tubesheet holes in CE designed units are classified as being either rough bore or smooth bored depending on the plant. The rough bore drilling process results in holes more like, but not necessarily identical to, those in Westinghouse designed SGs, also a drilling process, than the smooth bore trepanning process used for a few plants' SGs.

Most of the initial test program was conducted using specimens at ambient conditions, i.e., 70°F, with a few specimens tested at elevated temperature. All of the first series of tests used deionized water as the testing medium. A significant fraction of the specimens exhibited no leakage at pressures approximating normal operation and SLB conditions. The results of the tests were analyzed using the W* methodology for the Reference 5.6 presentation in response to an NRC query regarding whether the results obtained by Westinghouse were similar to those obtained by CE (now a part of Westinghouse). It was found that the loss coefficients from the C* tests were not inconsistent with those from the W* tests. This is an expected result since the explosive expansion process would be expected to be somewhat consistent, but not identical, from one SG fabricator to another. As noted above, it is possible that the finish results from the drilling process would also be different and the differences could affect the leak rate test results.

A second series of tests was initiated at the same time as the Model D5 testing program to increase the amount of data available at elevated temperature and to obtain results using primary water as the testing medium. A total of nine (9) specimens remaining from the initial test program were tested to obtain additional leak rate data points. The preliminary results from the analysis of the test data indicated an average decrease in the crevice resistance, i.e., loss coefficient, of about a factor of eight relative to the prior C* test data. Since the final results from the analysis of the data were not expected to be available for several weeks, one utility, with a plant in a SG inspection outage, decided to significantly increase the length within the tubesheet that would be inspected by RPC. Those results have not been finalized as of the time of this writing, however, there are no expected findings that would raise any concerns relative to the W* test program or its results.

5.3.4.3 Discussion

There have been several series of tests run to measure the resistance of the tube-to-tubesheet crevice for a variety of joints fabricated by both Westinghouse and Combustion Engineering. Most of the tests employed deionized water as the test medium but some of the recent tests employed a primary water simulant, borated and lithiated. Two sets of test results from the recent tests provided a direct comparison of results using DI water with those using borated and lithiated water. One set of those tests led to results indicating the later medium leads to reduced leakage relative to DI water while the other led to somewhat contradictory results. The first set was performed using test specimens simulating the hydraulic expansion of tubes into the tubesheet while the second simulated the CE explosive expansion process, a.k.a. expansion. Hydraulically expanded joints are looser than explosively expanded joints and offer less resistance to flow. In addition, models of the joint behavior would indicate that the W^* joint loss coefficient should exhibit a higher dependency, i.e., correlation slope, than that of H^* joints. The W^* results are totally consistent with these technically based expectations. In addition, the conduct of the W^* tests was such as to minimize any of dissolved oxygen in the testing medium.

There were some inconsistencies noted from the results of the second series of C^* tests. The leak rates were of similar magnitude to those obtained from tests of hydraulically expanded, i.e., H^* , joints. This is contradictory to physical expectation since explosively expanded joints have been verified to lead to a higher pullout resistance. This higher residual contact pressure results in a smaller leak path through the crevice and should result in a smaller leak rate for the same thermal and differential pressure conditions. In addition, the leak rates from the second series of C^* tests did not result in significant differences between smooth and rough bore tubesheet specimens. The first series of tests demonstrated a higher crevice leakage resistance for rough bore tubesheet samples. This is consistent with some models of the tube-to-tubesheet interface and how it is changed during the expansion process.

5.3.4.4 Conclusions

There is no direct evidence to suggest that any changes should be made to the W^* inspection length. Indeed, final analyzed test data, the H^* results, indicate that there should be no difference between results obtained with deionized or primary water. There are enough consistencies between the results obtained from the original W^* tests relative to the later H^* tests to conclude that the data were valid and formed an appropriate basis for establishing the W^* criteria values. There are inconsistencies noted with the C^* test results to conclude that they should not be used as a basis for modifying the W^* criteria. Information gathered regarding the conduct of the tests supports this conclusion. Thus, the direct evidence that is available confirms the validity of the W^* test results.

Finally, there are so few circumferential indications in the SQN2 SG tubes within the tubesheet that the margin relative to the allowable leak rate is very significant. The conclusion from these considerations is that the W^* criteria should not be modified for the SQN2 tube inspections (Reference 5.8).

Figure 5.1 WEXTEx Loss Coefficient as a Function of Added Contact Pressure



5.3.5 Address How Leak Model Addresses 360° Circumferential Crack (Callaway RAI # 17, 26, 31 and 37)

The bounding leak rate model is directly based on the test data from effectively severed tubes and thus obviates the concern that led to the original RAIs. The prediction of leak rates is discussed in Section 4.0 of this report. The leak rate from a 360° crack between at the W* distance and 12 inches below the top of the tubesheet at the worst case radial location within the tubesheet is calculated to be 0.0045 gpm at 90% prediction interval. At greater than 12 inches below the top of the tubesheet, the bounding per tube leakage allowance is approximately $9 \cdot 10^{-5}$ gpm. Modeling of future leak rates is a function of the number of circumferentially oriented cracks that are in the SGs at elevations below the W* distance.

5.3.6 Leak Rate Loss Coefficient RAI Discussion (Diablo Canyon RAI # 4 and 5)

The bounding leak rate model is directly based on the test data from effectively severed tubes and thus obviates the concern that led to the original RAIs. The response that was provided to support the application of W* at Diablo Canyon is provided for information.

5.3.6.1 Background

Mr. Phillip Rush, then of the NRC staff, transmitted a facsimile to Mr. Thomas Pitterle of Westinghouse on September 29, 1998, with the following discussion:

“Attached are copies of some Excel graphs I made to investigate the possibility of specimen dependence on the unusual scatter evident in Figure 6.4-2 of the W* topical report. I first separated the data into four groups by specimen ID, i.e., W4-001, W4-004, W4-008, and W4-018. Then I broke down the data in some of the groups into three subgroups (short, medium and long). Short medium and long specimens are those with crevice lengths on the order of 0.5 inches, 1 inch, and 2 inch respectively. As you can see from the attached figures, tests of W4-004 specimens and W4-018 clearly demonstrate that something unusual has cropped up in the test results. Please look at this and get back to me with your conclusions. Feel free to call me to discuss this observation.”

The facsimile from Mr. Rush looks at the data base used to establish crevice loss coefficients for WEXTEx tube-to-tubesheet crevices. This data base was developed from leak tests run on simulated WEXTEx crevices and appears as Figure 6.4.2 of Reference 5.4. The data set is listed in Table 6.2-3 of Reference 5.4.

The information plots transmitted by Mr. Rush depicted data from Reference 5.9, which was prepared in response to earlier RAIs and updated Table 6.2-3 of the WCAP to include calculated loss coefficients (flow resistance) for the test specimens. The essence of Mr. Rush’s concern is summarized as “... tests of W4-004 specimens and W4-018 clearly demonstrate that something unusual has cropped up in the test results.”

The “something unusual” to which Mr. Rush refers is apparently that the loss coefficient appears to be dependent on crevice length. Physically, the loss coefficient should be independent of the length of the crevice.

5.3.6.2. Purpose

A review the WEXTEx leak rate data set and resulting calculated loss coefficients was conducted to determine if an unwarranted crevice length effect on loss coefficient is evident in the test data (Reference 5.9).

5.3.6.3 Loss Coefficient vs. Contact Pressure (Diablo Canyon RAI #4 and # 5)

Mr. Rush re-plots the data set of loss coefficient vs. contact pressure (Figure 6.4-2 of Reference WCAP-14797-P, Rev 2). The loss coefficient test data used by Mr. Rush were provided via Reference 5.9. A review of the data set in this letter shows that most of the loss coefficients are an order of magnitude higher than those plotted on Figure 6.4-2. The corrected data set is attached as Table 5-4 to this letter and supercedes the data set previously provided via Reference 5.9. It is noted that Table 5-4 represents the data analyzed in support of the conclusions of Reference 2.1.

Mr. Rush’s plots of the data, separated by sample number and crevice length, were re-plotted using the correct data set. These plots appear as Figures 5.2 through 5.5. Except for a few of the points, the plots have the same appearance as Mr. Rush’s with the loss coefficient scale an order of magnitude lower. The data scatter on Figures 5.2 through 5.5 is consistent with the scatter on Figure 6.4-2 of Reference 5.4. Recall that the data appear to have constant variance about the regression line of Reference 5.4 and do not contradict the assumption of normality for the distribution of the residuals from the regression analysis.

On the surface, Figure 5.3 (for Sample W4-004) and to a lesser degree, Figure 5.5 (for Sample W4-018) seem to indicate that loss coefficient is increasing with decreasing crevice length. Samples W4-001 and 008 do not show this pattern. Figures 5.6 through 5.9 re-plot the same loss coefficient data sets versus crevice length with operating conditions as a parameter. When viewed in this manner, the data shows no consistent trend of loss coefficient variation with length. Sample WP4-001 shows a general increase of loss coefficient with length although one set of operating conditions shows the reverse trend. The medium lengths for Sample WP4-004 have lower loss coefficients than the short lengths, but the trend is reversed for the single set operating conditions tested at the long length. Sample WP4-008 shows a general increase of loss coefficient with length. Sample WP4-018 shows a decrease of loss coefficient with length for the medium and long lengths, but the reverse trend for the single case of short and medium length tested.

5.3.7.4 Conclusions

The above review of the loss coefficient data for WEXTEx crevices shows no consistent length effect. The absence of a length effect is expected based on physical grounds.

Overall, it is noted that the leak rate data include considerable scatter, but do not show unacceptable bias toward the variables influencing crevice leakage. While scatter is common for leak rate data, the W* tests may include more than typical data scatter. The leak rates are small and minor variations in the crevice can influence the observed leak rates. Regardless, the spread in the loss coefficient data and associated uncertainties on the leak rates are included in the W* analyses, for both the loss coefficient and effective crack length.

5.3.7 Evaluation of Axial PWSCC within W* Distance (St. Lucie RAI # 17 and Callaway RAI # 72)

SLB Conditions Leakage Potential from Axial PWSCC within W*

At the BVPS 1R15 outage, 18 axial PWSCC indications on 18 tubes were reported. These indications ranged in elevation from 0.18 inch below TTS to 9.79 inch below TTS. The breakdown of indications per SG was; SGA, 3, SGB, 5, SGC, 10. Ten (10) of these 18 indications were noted within 1 inch of the TTS, and are assumed to be located within the expansion transition. The largest amplitude signal of 1.89 volts by +Pt was noted on tube R20 C36, SGA. Based on a +Pt amplitude versus depth correlation developed by Westinghouse, the maximum depth of this indication is estimated at 71%TW. The phase based depth analysis indicated a maximum depth of 97%TW. This flaw was located at 0.43 inch below TTS, which locates it within the expansion transition, and this elevation report is also consistent with the measured BWT. As this indication was located so close to the TTS, if it truly contained 100%TW penetration, leakage would be expected. The flaw length from profiling was 0.31 inch. This indication was in situ pressure tested to 2841 psi with no leakage and no burst reported at 4900 psi. FENOC has conservatively performed in situ pressure testing at previous outages of other axial PWSCC indications located within the W* distance. At the 1R14 outage (2001), a 1.98 volt axial PWSCC indication located at 1.86 inch below TTS was in situ pressure tested with no leakage or burst reported. At Diablo Canyon, axial PWSCC indications with amplitudes up to 5.6 volts by +Pt have been in situ pressure tested with no leakage or burst reported. At 5.6 volts, this indication is judged to have contained a 100%TW penetration. No less than 5 of the in situ pressure tested indications at Diablo Canyon are judged to have contained a 100%TW penetration based on +Pt amplitude. None leaked during in situ pressure test.

Other industry in situ pressure test data supports the application of the voltage based sizing technique. During the Fall 2003 inspection at a plant with C-E SGs, a 1.9 volt by +Pt, 106° arc length circumferential PWSCC indication was reported at the top of tubesheet. The phase based depth assessment indicated that the maximum depth of 99%TW extended for nearly the entire flawed length. This indication was in situ pressure tested for leakage only. No leakage was reported at 2900 psi. It should be noted that the depth estimate using the amplitude correlation is approximately 73%. In conclusion, in situ pressure testing of PWSCC indications at or below TTS has shown no leakage potential for indications up to 5.6 volts by +Pt.

Growth of Non-Detected or New Initiates During Operation

A history review of each of the BVPS 1R15 indications was performed using the 1R14 +Pt inspection data. Thirteen (13) of the 18, 1R15 flaws had a precursor signal in the 1R14 data. Of the five 1R15 indications with no precursor signal in 1R14, only one had an amplitude >1V. This indication was found at 0.49 inch below TTS, placing it within the expansion transition. The only indication with a modest amplitude growth was R20 C36, which had an amplitude growth of 1.38 volts. As this indication was located within the expansion transition, the higher residual stresses of the transition would be expected to exacerbate growth. R20 C36 also had the largest length growth of 0.14 inch, and also had the only substantial depth growth (by phase) of 59%. Cycle 15 growth data is provided in Table 1. The Cycle 14 growth statistics are essentially equal to the Cycle 15 growth statistics. The only appreciable difference between the growth data for Cycles 15 and 14 is maximum depth growth. The expansion transition flaws appear to have a slightly higher maximum depth growth. The average +Pt voltage growth of 0.31 volts is modest for PWSCC as PWSCC amplitudes are greater than ODSCC for equal depths. The average length growth of 0.01" suggests that the residual stress fields that initiate the PWSCC are limited in length and do not represent a potential for indications with significant lengths.

The average +Pt voltage of the 1R14 precursor signals was 0.52 volts, suggesting that the detection threshold for axial PWSCC is slightly above this value. With a maximum +Pt voltage growth for Cycle 15 of 1.38, the maximum EOC16 PWSCC amplitude expected is approximately 2 V. Based on the correlation of +Pt voltage to maximum depth, this postulated indication would be expected to have a maximum depth of about 74%TW. Therefore, axial PWSCC within the W* distance that either is initiated during the cycle or remains in service based on probability of detection is judged to result in an indication that is well <100%TW at the end of the next operating cycle, and will not contribute to primary to secondary leakage during a postulated SLB event. If 1R16 observed axial degradation within the W* distance is judged to contain 100%TW penetration, the end-of-cycle 17 evaluation of postulated SLB condition leakage will account for these indications in the calculation of SLB leakage in the operational assessment.

Indication Distribution

Approximately half of the total reported indications occur within 1 inch of the top of tubesheet. A regression of all indication elevations and number of indications within a 1 inch elevation bin produces a best fit curve that predicts approximately 2 indications in the 8 to 9 inch below TTS bin, and approximately 1 indication per bin at 12 inches below TTS and lower. A regression was fit using all data with the exception of the data in the TTS to 1 inch below bin to determine if the initiation trend follows a similar pattern as for all data. The regression for this subset of data is essentially equal to the regression for all data. Thus, the judgment that the flaw initiation potential decreases with increasing depth below TTS remains valid for this data. Figure 4.5 presents the plot of all data and below expansion transition data as a function of depth below TTS. Note that the 90% probability prediction interval for all data bounds the data, particularly at the deeper elevations (Figure 4.5).

5.3.8 Contact Pressure Throughout the SLB Event (Callaway RAI # 61)

Information provided to the NRC during the June 8, 2004 meeting plots contact pressure as a function of depth below TTS for the SLB event at 4200 seconds. WCAP-14797 presents a summary of contact pressures for various conditions. Using the WCAP-14797 information for normal operating conditions, the Zone B contact pressure at 8" below TTS is approximately 1406 psi, with WEXTEX contact pressure included. However, this calculation assumes a hot leg temperature of 590°F and also assumes that the secondary side pressure (assumed 900 psi) acts on the tube OD over the entire tube in tubesheet length. For the SQN2 condition, additional contact pressure will be provided due to the actual hot leg temperature of 609.5°F. The drilled hole leakage test data suggests that the pressure drop through the actual crevice length of 2.25 inch is about 2500 psi based on the observation that 2 of the 4 samples had no leakage during the leak test with a 2650 psi pressure differential. Thus, the assumption that the secondary pressure acts on the tube OD in the crevice without losses is quite conservative. If secondary side pressure does not act on the tube OD in the crevice at deep depths, which is a reasonable assumption, and the actual hot leg operating temperature and pressure differential for SQN2 is applied, the normal operating contact pressure at the tubesheet neutral axis is approximately 2403 psi, which bounds the contact pressure of the 3 inch nominal samples. The SLB reference case for contact pressure evaluation used a hot leg temperature of 460°F and pressure differential of 2560 psi. The neutral axis contact pressure for the SLB case at 4200 seconds is approximately 2903 psi, which also bounds the contact pressure of the 3 inch nominal samples.

Contact pressures at the neutral axis were also evaluated for the Case (3) condition of Table 3.2-1 of WCAP-14797. This case considers plant conditions at 600 seconds into the SLB event. For this case the hot leg temperature is 433°F, the secondary side temperature is 212°F, and primary to secondary pressure differential is 2344 psi. The contact pressure at the neutral axis is 2683 psi, which still bounds the contact pressure of the 3 inch nominal leakage samples by approximately 600 psi. These calculations were performed using the same model used to develop the contact pressures contained in WCAP-14797, only the input values were changed to account for the different temperatures and pressures. These calculations were performed for a depth below TTS of 10.5 inch. The bounding leakage methodology presented to the NRC on June 8, 2004 compares contact pressures at 12 inch below TTS against the 3 inch nominal leakage samples. The actual tube contact pressures at 12 inch below TTS will be several hundred psi greater than the values listed above. Therefore, the bounding leakage methodology is judged to be conservative for the SLB event. While the leakage tests were conducted at 600°F and the 4200 second SLB hot leg temperature is predicted to be 460°F, the results of the leakage test are still considered applicable as flashing of the primary water in the crevice is expected to occur at both 600°F and 460°F, thereby resulting in a choked flow condition. Note that the measured, condensed mass flows are essentially equal for the range of pressure differentials, suggesting a potential for a choked condition. The contact pressure model calculates contact pressures at the neutral axis (10.5" below TTS), 6, 4, and 2" below TTS as well as at TTS. For the 6 inch below TTS elevation for hot leg temperature of 433°F, secondary side temperature of 212°F, and 2344 psi differential pressure, the contact pressure is 1803 psi. The bounding leakage model considers a separate leakage allowance for postulated separated tubes at 8 to 12" below TTS as well as >12" below TTS. Therefore, at 8" below TTS, the contact pressure is expected to be approximately 2194 psi (interpolation using 6 inch and 10.5 inch below TTS contact

pressures), which is well above the contact pressure of the 1.25 inch nominal leakage samples of approximately 1352 psi. Therefore, the bounding leakage methodology is judged to be conservative for the SLB event for both the 8 to 12 inch below TTS elevation and the >12 inch below TTS elevation.

Table 5-4
WEXTEX Loss Coefficient Reanalysis
Arranged by Sample #/Crevice Length

a,c,e

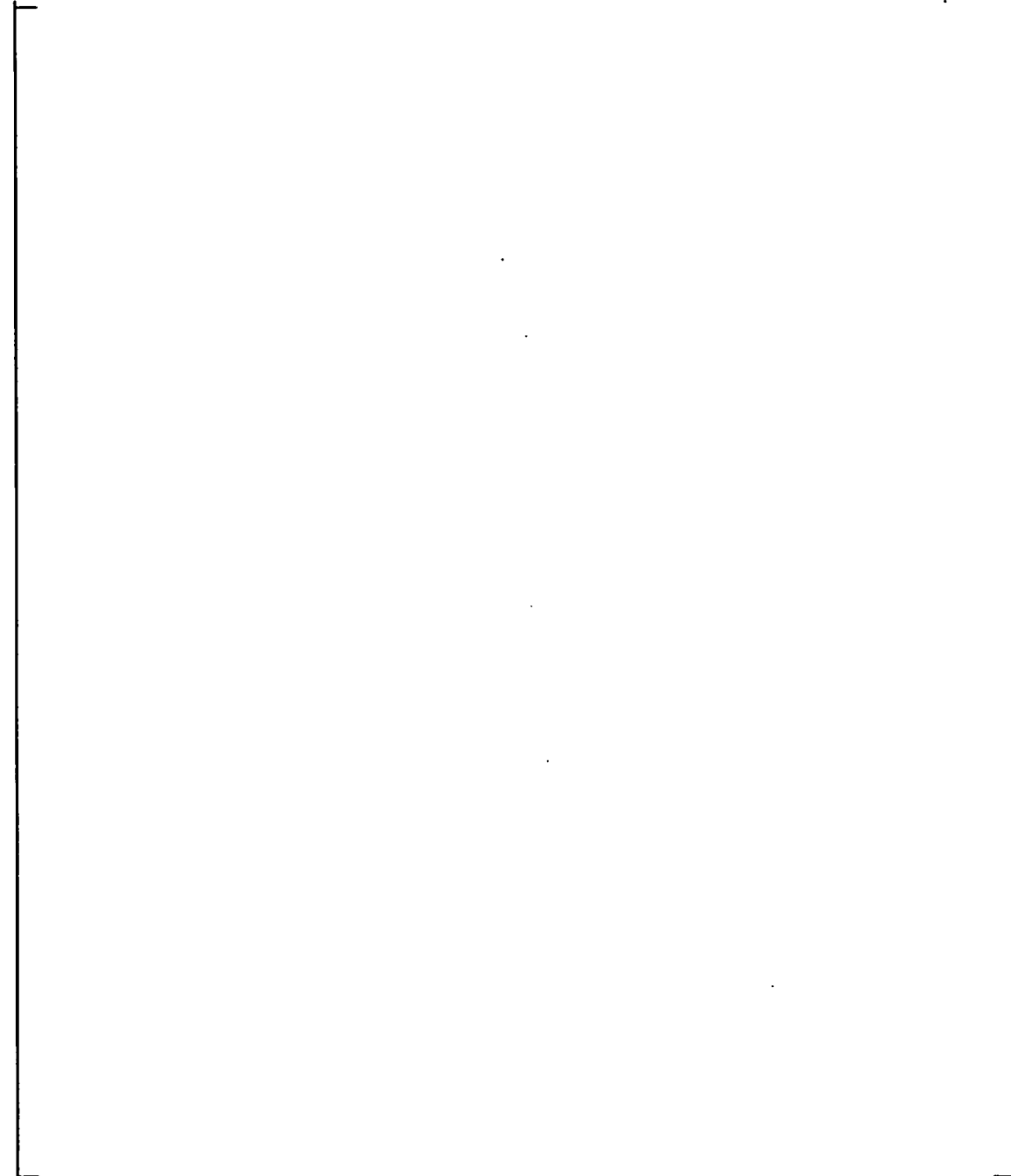


Figure 5.2 Loss Coefficient vs. Crevice Length – Sample W4-001

a,c,e



Figure 5.3 Loss Coefficient vs Contact Pressure – Sample W4-004

a,c,e

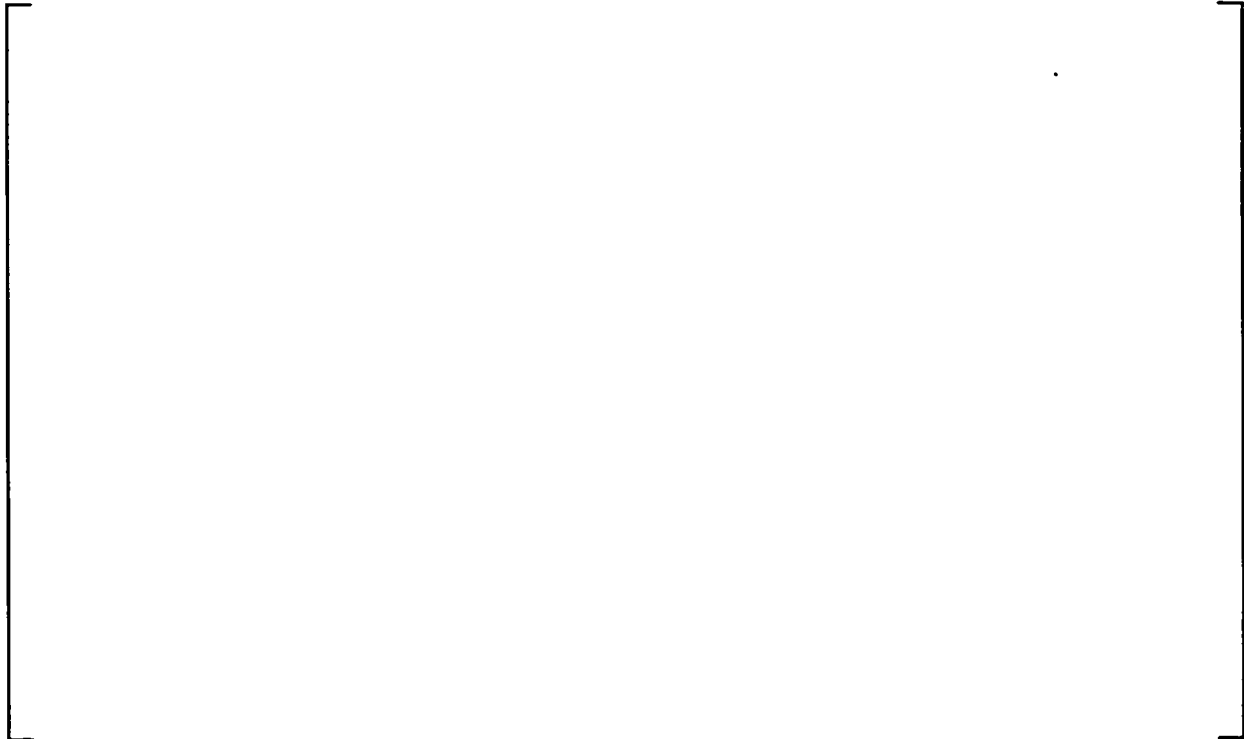


Figure 5.4 Loss Coefficient vs. Crevice Length Sample W4-008

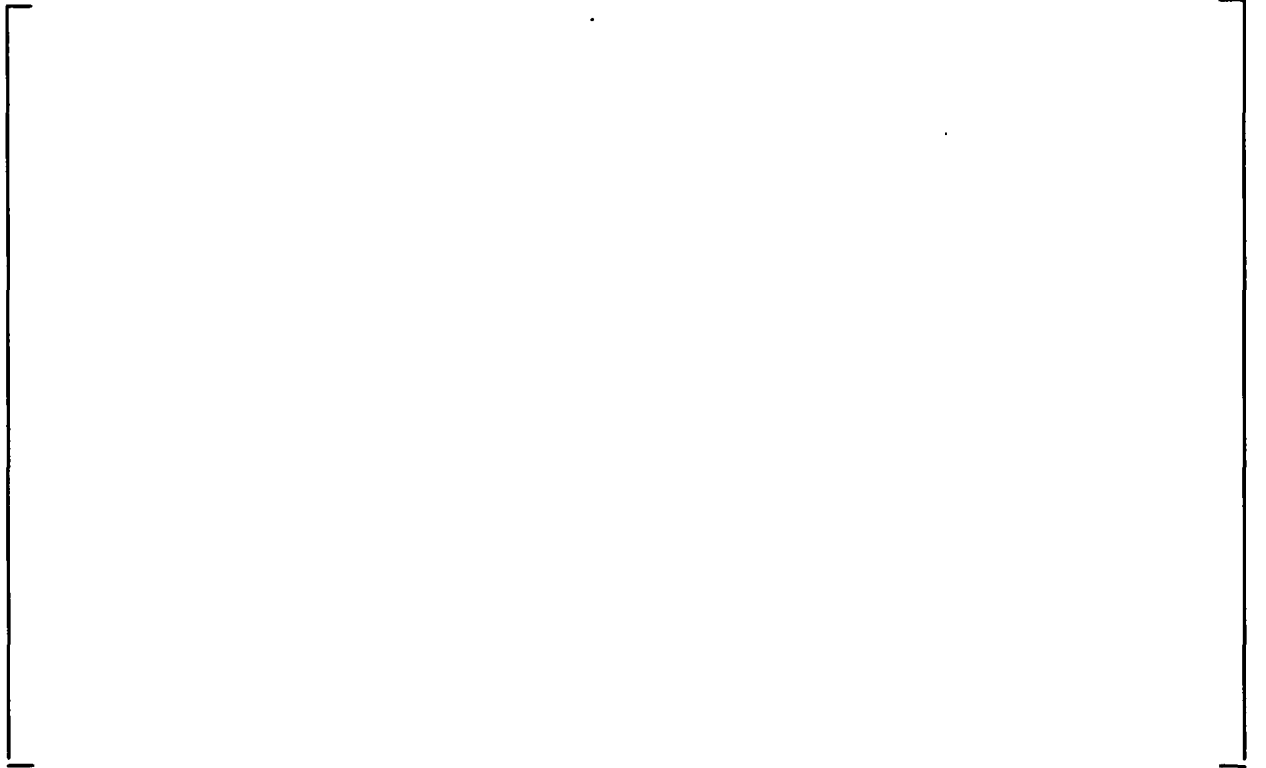


Figure 5.5 Loss Coefficient vs. Contact Pressure –Sample W4-018



Figure 5.6 Loss Coefficient vs. Crevice Length



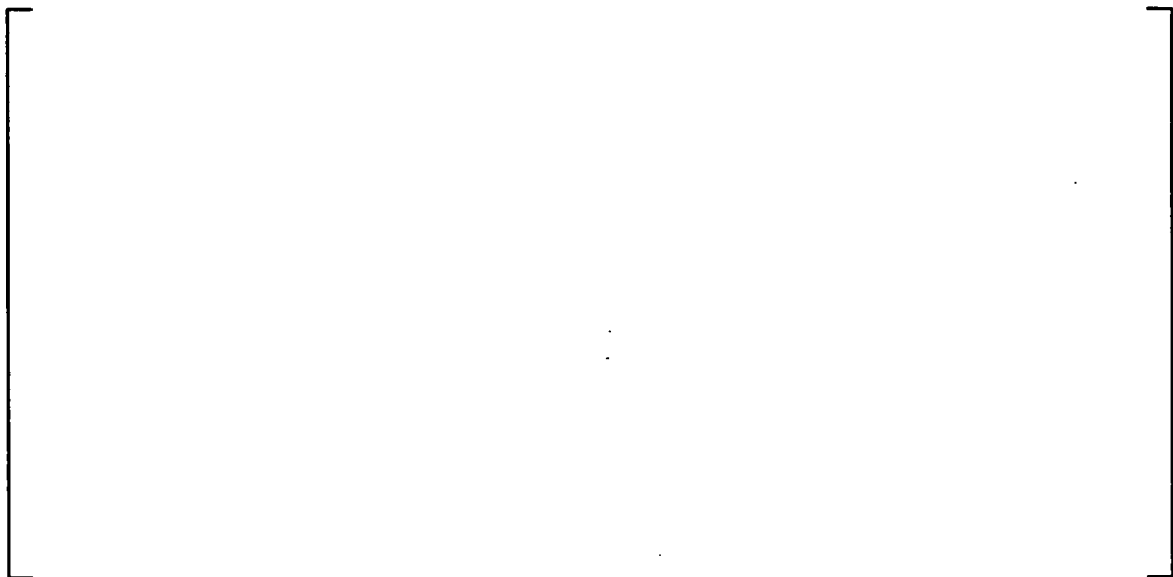
Figure 5.7 Loss Coefficient vs. Crevice Length Sample WP4-004



Figure 5.8 Loss Coefficient vs. Crevice Length



Figure 5.9 Loss Coefficient vs. Crevice Length



5.4 REFERENCES

- 5.1 NSD-E-SGDA-98-017, "RAI for Application of W* Tube Repair Criteria at Diablo Canyon," 1/26/98
- 5.2 CN-SGDA-04-52, "W* Ligament Tearing for Model 51 Steam Generators at Beaver Valley Unit 1," 5/19/04
- 5.3 NSD-E-SGDA-98-260, Rev. 1, "Response to NRC RAIs on Diablo Canyon W*," 8/20/98
- 5.4 WCAP-14797 (Proprietary), Revision 2, *Generic W* Tube Plugging Criteria for 51 Series Steam Generator Tubesheet Region WEXTEx Expansions*, Westinghouse Electric Company, Madison, PA (March 2003)
- 5.5 WCAP-14795 (Proprietary), *NRC/Utility Meeting on Model 51 Steam Generator Tube Integrity ARC Methodology*, Westinghouse Electric Company, Madison, PA (December 1996).
- 5.6 Presentation Material, "The Application of W* Criterion to TVA SGs at Sequoyah Nuclear Station," Tennessee Valley Authority Meeting with the NRC Staff, Rockville, MD (September 10, 2003).
- 5.7 LTR-SGDA-04-104, "Clarification of W* Leak Rate Testing," Westinghouse Electric Company, Nuclear Services Division, Madison, PA, April 29, 2004.
- 5.8 PGE-04-24, "Pacific Gas and Electric Company Diablo Canyon Units 1 and 2, W* Implementation Recommendation," 3/12/04
- 5.9 NSD-E-SGDA-99-006, "NRC RAI on Diablo Canyon W* Loss Coefficient," Westinghouse Electric Company, Nuclear Services Division, Madison, PA, January 11, 1999.